Arabian Journal for Science and Engineering (2019) 44:6465–6487
https://doi.org/10.1007/s13369-019-03778-x

RESEARCH ARTICLE - EARTH SCIENCES

Sedimentological and Geochemical Analysis of the Middle Jurassic Shinawari Formation, Upper Indus Basin, Pakistan: Implications for Palaeoenvironmental and Hydrocarbon Assessment

Fahad Ali[1,2] · Jin Qiang[1] · Sajjad Ahmad[3] · Suleman Khan[3] · Muhammad Hanif[4] · Irfan Ullah Jan[4]

Received: 20 July 2018 / Accepted: 12 February 2019 / Published online: 26 February 2019

Abstract
Microfacies, palynofacies, and hydrocarbon source rock potential of Toarcian–Bathonian sediments of the Shinawari Formation are investigated in the Chichali Nala Section, Baroch Nala, Gulla Khel Nala, Surghar Range, and Askari Cement Factory Section, Nizampur Kala Chitta Range, Pakistan. The Shinawari Formation is dominated by a mix of limestone, sandstone, shale, marls, siltstone, and mudstone units with the association of laterite, hard grounds, coal layers, and coal disseminations. Microfacies analysis suggests that deposition of the Shinawari Formation occurred in peritidal lagoon, beach shoal to distal shelf setting. This interpretation is supported by sub-types of standard Tyson (in: Sedimentary organic matter, Springer, Berlin, 1995), palynofacies, which we have defined as palynofacies SFPF-A, attributed to a marginal dysoxic to an anoxic basinal setting, and palynofacies SFPF-B, deposited in heterolithic proximal platform settings. Some of the intervals have low ($\leq 0.5\%$) total organic carbon (TOC) values except for intervals with fair values (0.5–2.09%) in the Shinawari Formation in different stratigraphic sections. Despite some lower TOC values, and the presence of kerogen types III and II, spore colouration index of 5.0–8.0, thermal alteration index of 2–3+, and vitrinite reflectance (VR) of 1.16–1.35 indicate possible hydrocarbon source rock potential. The various geochemical plots obtained from TOC (%), VR and Rock-Eval pyrolysis data indicate that the Shinawari Formation specifies kerogen type III having Tmax (°C) range of 430–450°C and thermal maturity lies in the oil window.

Keywords Shinawari Formation · Indus Basin · Pakistan · Palynofacies · Microfacies · Source rock

1 Introduction

The Indus Basin of Pakistan lies between the Main Boundary Thrust separating the metamorphic sub-Himalaya in the north and the Arabian Sea in the south-west. The basins are structurally subdivided into the Upper, Central, and Southern Indus Basin, each containing sedimentary rocks from Precambrian to Tertiary and a petroleum producer [2,3]. The Upper Indus Basin hosts a fairly complete Mesozoic succession containing shallow-water carbonates with siliciclastics that were deposited at palaeolatitude ~20° to 30° South [4,5] and include the subject of this study (Figs. 1, 2). The Jurassic Shinawari Formation was first discussed by Fatmi [2] for the transition zone between the underlying Datta and the overly-

✉ Fahad Ali
fahadalizai@bkuc.edu.pk; fahadalizai@outlook.com

Jin Qiang
jinqiang@upc.edu.cn

Sajjad Ahmad
dr.s_ahmed@uop.edu.pk

Suleman Khan
sulemanafridi@uop.edu.pk

Muhammad Hanif
hanif.nceg@gmail.com

Irfan Ullah Jan
irfanjan6@gmail.com

[1] School of Geosciences, China University of Petroleum East China, Qingdao, China

[2] Department of Geology, Bacha Khan University, Charsadda, Pakistan

[3] Department of Geology, University of Peshawar, Peshawar, Pakistan

[4] NCE in Geology, University of Peshawar, Peshawar, Pakistan

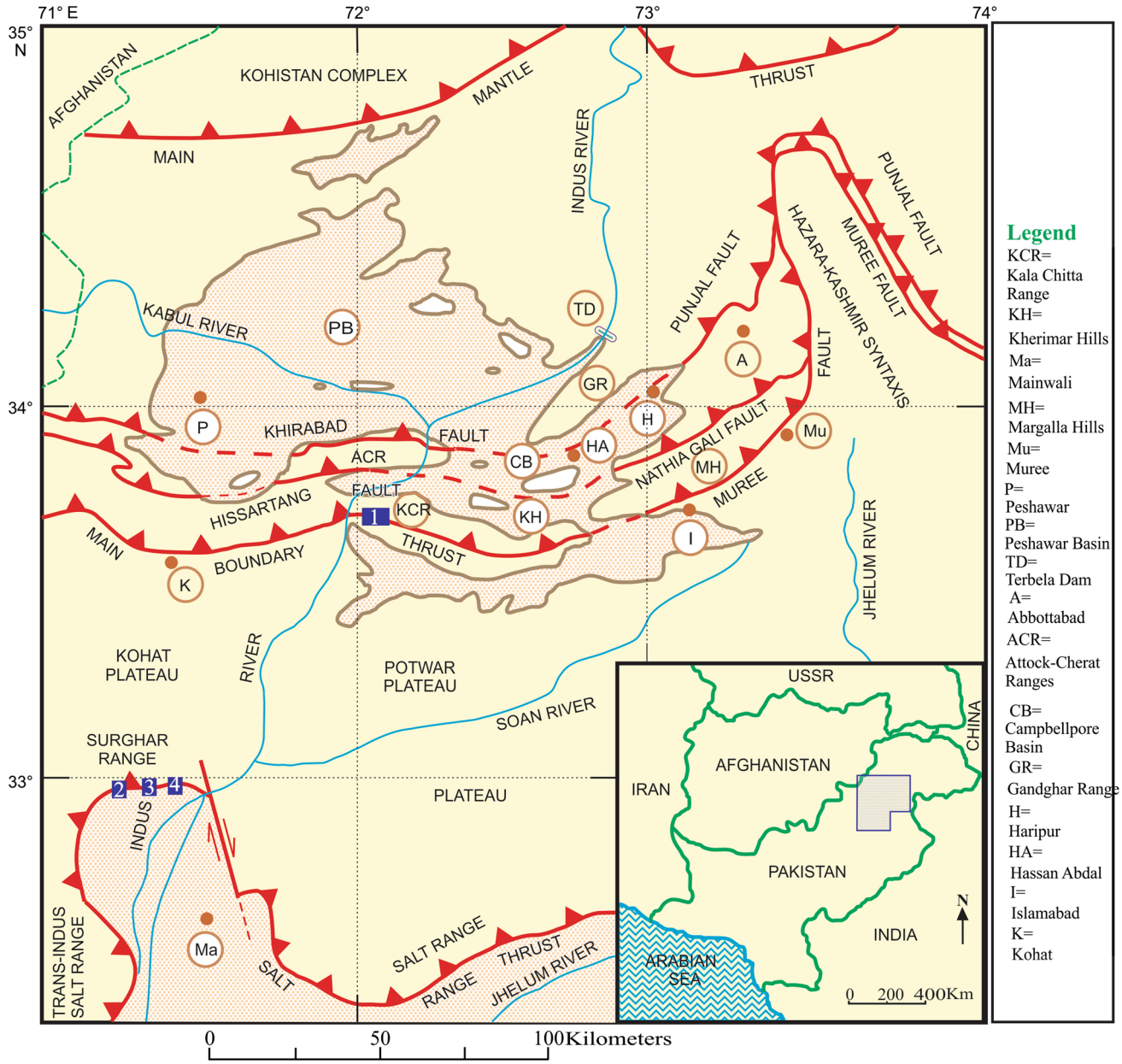

Fig. 1 The location of Shinawari Formation, in (1) Nizampur Section; (2) Baroch Nala; (3) Gula Khel Nala; and (4) Chichali Nala Section, Upper Indus Basin, Pakistan

ing Samana Suk Formations, in the western Samana Range, Kohat Plateau, Pakistan. Different exposures of the Jurassic rocks have been studied in the Salt Range and Trans Indus ranges in the context of sedimentation, sequence stratigraphy, and biostratigraphy by previous workers [2,6–11]. Ahmed et al. [9] studied the whole Jurassic sequence in Surghar and Salt ranges in the broader context of sequence stratigraphy and sedimentology, focusing on the Shinawari and Samana Suk Formations, which portray a generalized picture depositional settings of these formations based on microfacies analysis. Published literature on the microfacies, lithofacies, palynofacies, and geochemical source rock integrated analysis for the depositional setting and source rock potential of the Shinawari Formation is scarce to non-existent. Our source rock evaluation is based on a broad range of methodologies, that is to develop a basin model deduced from various rock properties such as detailed litho-, micro-, and palynofacies with geochemical analysis. In addition to the conventional use of microfacies analysis, palynofacies and geochemical analyses are used in the development of basin analysis and production of geologic models. Palynofacies analyses provide direct qualification and quantification of organic source

rock material in the studied units. In addition to source rock properties, it can indicate organic matter provenance, palaeobiology, and sedimentary dynamics [12–16]. This paper aims to integrate litho-, micro-, and palynofacies along with the source rock geochemistry of the Shinawari Formation in the Upper Indus Basin, to understand its palaeoenvironments and hydrocarbon source rock potential.

2 Methods

The present work covers detailed stratigraphic logging of the Shinawari Formation exposed in the Chichali Nala, Baroch Nala, and Gula Khel Nala of the Surghar Range, Mianwali District, and the Askari Cement Factory Section in Nizampur, Nowshera District, Pakistan (Fig. 1). Variations in colour, texture, fossil content, and lithology are used to construct a composite stratigraphic log. The Shinawari Formation was measured, logged, and sampled in the above-mentioned field sections. Stratigraphic thicknesses of the Shinawari Formation are recorded ranging from 30 (Baroch Nala) to 125 m (Chichali Nala) (Figs. 3, 4, 5, 6). Thin sections were prepared from limestone and sandstone and were studied under the microscope. The limestone and sandstone are classified using the Dunham [17] and Folk [18] classification schemes. Palynological slides were prepared from organic-rich shale intervals following the technique of Wood et al. [19]. Pollen and spores observed in these samples were studied and identified using transmitted light microscopy according to the procedure described by Steffen, Gorin [20], and Khan [21].

For more accurate documentation of palynofacies and source rock characteristic, 300 counts of palynodebris were performed by traversing along the length of the slides. Epifluorescence (EF) microscopy was carried out through a Nikon SMZ25 microscope with blue light excitation (near UV) to study the amorphous organic matter (AOM). A Nikon OS-F12 polarizing microscope was used to photograph the AOM and other petrographic attributes. The standard recommendations of Tyson [1] are used for EF palynofacies examination for kerogen classification following Dow and O'Connor [22], Krevelen [23], Bordenove et al. [24], and Langford and Blanc-Valleron [25]. Hydrocarbon source rock potential was evaluated on the basis of total organic carbon (TOC), Rock-Eval pyrolysis, along with thermal alteration index (TAI), spore colour index, and vitrinite reflectance [26–29]. Quantitative estimation of the organic matter was made by visual estimation and the classification described by various researchers [1,13–15,22,30].

3 Results and Discussion

3.1 Litho- and Microfacies and Palaeoenvironments

3.1.1 Restricted Lagoon (MFT 1)

The MFT 1 is subdivided into two sub-facies MFT 1(A) and MFT 1(B).

Description

The lime mudstone microfacies (MFT 1(A)) at outcrop scale is represented by light grey, black to maroon argillaceous limestone on a fresh surface, and yellowish brown on the weathered surface. It is thin to medium bedded (Fig. 2). The MFT 1 microfacies stratigraphic thickness and vertical repetition in different studied stratigraphic sections are discussed in Table 1. It consists of calcareous lime mud matrix, with allochems of ostracods and sponge spicules (< 2%), non-skeletal allochems including pellets (3%), and fine-grained quartz (2%). Pervasive dolomitization is seen as the diagenetic product (Figs. 3, 4, 5, 6, 8a, b).

The Peloid–Pelletal wackstone microfacies (MFT 1(B)) is represented by thin- to medium-bedded limestone interbedded with organic-rich black shales. The limestone shows burrows and secondary pyrite nodules at places. Under the microscope, this microfacies is characterized by the presence of pellets–peloid (30%), intraclasts (10%), skeletal allochems. The skeletal allochems are represented by crinoids (4%), brachiopods (2%), bivalves (2%), sponge spicules (2%), foraminifera (3%), and gastropods (1%). Micrite dominates the matrix; however, sparite and recrystallized calcite crystals are also commonly found (Figs. 3, 4, 5, 6, 8c, d).

Interpretation

The MFT 1(A) is represented by fauna, and non-skeletal allochems present in this microfacies are commonly found in the restricted area of the inner shelf; the very fine size and angular shape of quartz grains are considered to be carried as wind-blown particles to the low-energy depositional environment. This MFT 1(A) is similar to SMF-19 of Wilson [31] and represents deposition in a low-energy restricted lagoon setting [32] (Fig. 7).

The MFT 1(B) is represented by the existence of pellets–peloid, bivalves, brachiopods, foraminifera, and crinoids/echinoids suggesting deposition in a shallow-marine shelf environment with low salinity [33], while sponge spicules indicate slightly low-energy shallow- to a deep-marine depositional setting. The presence of intraclasts indicates high-energy condition which may be due to the wave and current activity in shallow-marine shelf environment. The MFT 1(B) is comparable with the SMF-19 of Wilson [31], representing a low-energy lagoon semi-restricted condition of inner shelf settings [32] (Fig. 7).

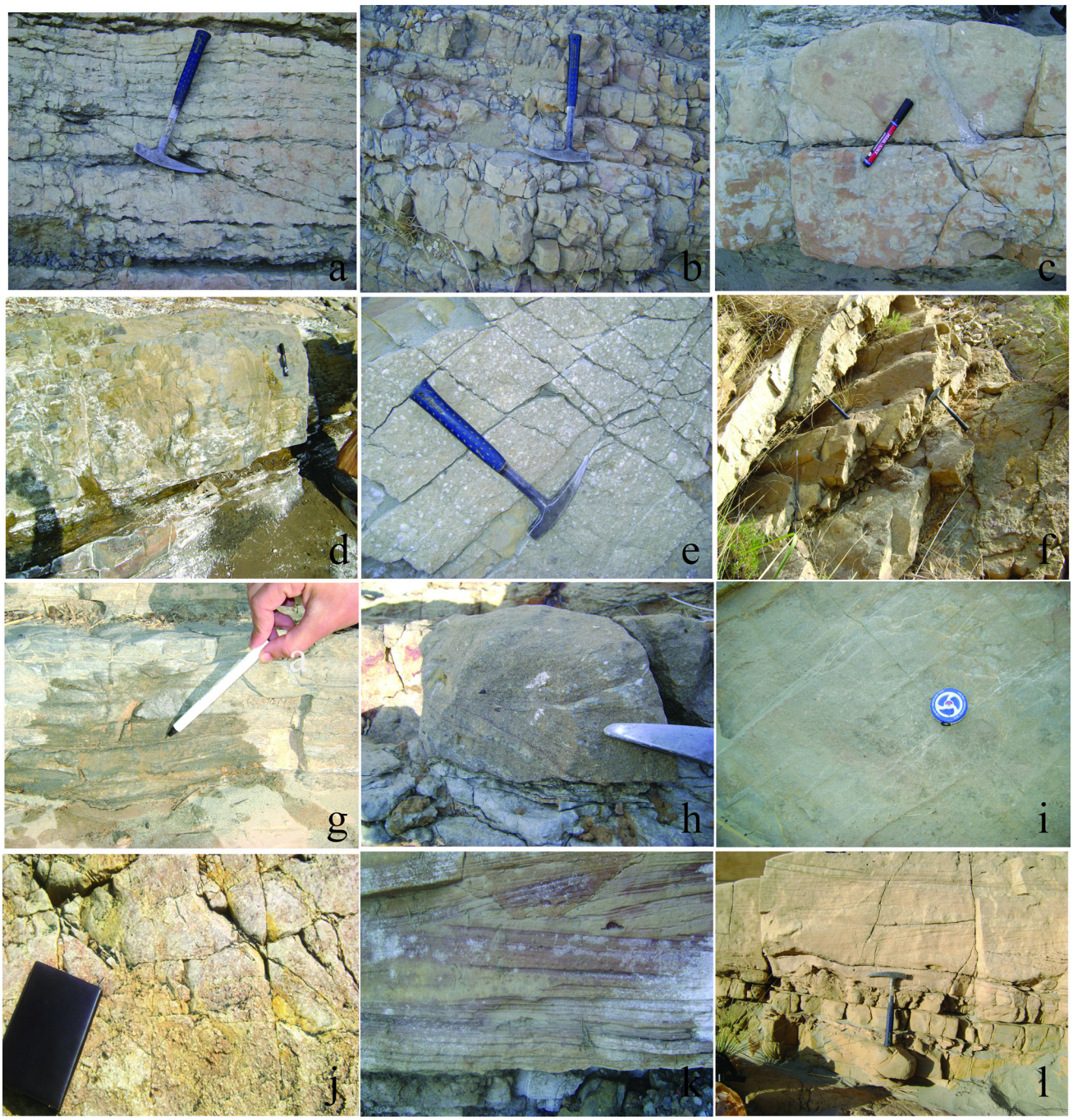

Fig. 2 Field photographs of Shinawari Formation at Upper Indus Basin displaying different MFTs field features such as MFT 1 (**a**, **b**), MFT 2 (**c**, **d**), MFT 3 (**e**–**h**), MFT 4 (**i**, **j**), LFT 1 (**k**, **l**)

3.1.2 Shallow-Marine Shelfal Setting (MFT 2)

Description

The wackstone microfacies (MFT 2) is comprised of greyish bedded limestone. The limestone is hard, compact, micritic, and unfossiliferous (Fig. 2). The stratigraphic thickness and vertical repetition of MFT 2 microfacies are represented in Table 1. The facies is composed of quartz (15%), worm burrows (10%), crinoids (8%), ooids (6%), brachiopods (4%), and micrite as a matrix. Some bioclasts are recrystallized to well-developed calcite crystals having well-preserved cleavage planes. Quartz is coarse grained and randomly arranged with rounded, smooth outlines, and having sub-spherical to elongated shapes. Ooids are completely spherical with radial and concentric fabric, while some ooids

Table 1 The stratigraphic thickness and vertical repetation of Shinawari Formation in Upper Indus Basin, Pakistan

Facies types		Stratigraphic thickness in Nala	Representative thin sections
MFT 1	A	Chichali Nala = 38 m	CS = 09, 12, 14, 16, 40, 58,
		Baroch Nala = 7 m	BS = 1–6,
		Gulla Khel Nala = 5 m	GS = 7, 13–14,
		Askari Cement Factory Sections = 37 m	NS = 6–7, 9–10, 11–12, 14–15
	B	Chichali Nala = 09 m	CS = 04, 12, 18, 19
		Askari Cement Factory Sections = 18 m	NS = 3–4
MFT 2		Chichali Nala = 1 m	CS = 02,
		Baroch Nala = 6 m	BS = 10, 15,
		Askari Cement Factory Sections = 13 m	NS = 4, 5
MFT 3		Chichali Nala = 22 m	CS = 3, 10, 21, 23, 24, 25
		Gulla Khel Nala = 7 m	GS = 6, 19
MFT 4	A	Chichali Nala = 4 m	CS = 22
	B	Gulla Khel Nala = 3 m	GS = 1
		Askari Cement Factory Sections = 5 m	NS = 1
LFT 1		Chichali Nala = 4 m	CS = 14b
		Gulla Khel Nala = 13 m	GS = 8, 12, 17,18
		Baroch Nala = 15 m	BS = 7, 8, 12, 14,
LFT 2		Chichali Nala = 5 m	No petrographic description
SFPF-A		Chichali Nala = 19 m	CS = 1–4, 6–9, 11–14
		Gulla Khel Nala = 16 m	GS = 2–6, 9–11, 20
		Baroch Nala = 2 m	BS = 9, 11
		Askari Cement Factory Sections = 2 m	NS = 8, 10, 13
SFPF-B		Chichali Nala = 22 m	CS = 5, 10,15, 16–20
		Gulla Khel Nala = 11 m	GS = 12, 15

are elongated with bioclasts as a nucleus (Figs. 3, 4, 5, 6, 8e, f).

Interpretation

The ooids are important palaeoenvironmental indicators for water energy, water depths, water salinity, and temperature of oceanic water. The concentric ooids are formed in shallow-marine, high-energy settings, i.e. oolitic shoals, tidal bars, and beaches [34–36]. The radial ooids usually formed in moderate- to low-energy settings such as lagoonal and sea marginal or lacustrine environments [36]. The salinity tolerance of echinoderms ranges up to few ppm, so they most commonly occur in marine geological setting, i.e. open shelf [33]. Worm burrows are formed on the shelf when the clastic input from near-beach areas influx into the environments and marine fauna are unable to survive. This microfacies is comparable with the SMF-9 of Wilson [31] and Flugel [37], representing the shallow-marine inner shelf to sand shoal beach environment (Fig. 7).

3.1.3 Open-Marine Shoals (MFT 3)

The intraclastic grainstone microfacies (MFT 3) is comprised of alternating beds of limestone and siltstone. The limestone is medium bedded, argillaceous, micritic, hard, and compact in nature. The grainstone texture can be observed in the field along with the planer and cross-bedding, ripples mark, and fossil imprints (Fig. 2). The stratigraphic thickness and vertical repetition of this microfacies are explained in Table 1. This microfacies consists of 31% intraclasts, 18% peloids, 17% quartz, 10% echinoids, 7% brachiopods, 5% ooids, 3% foraminifera, 3 % gastropods, 1% algae, and 1% bryozoans. The quartz is fine to coarse grained, having smooth outlines and elongated to sub-spherical shapes, and they are unsorted, ungraded, and having no pronounced contact boundaries. Different sub-types of intraclasts (simple and compound) are present which are poorly sorted, micritic, and angular to sub-rounded shape (Figs. 3, 4, 5, 6, 8g, h).

Interpretation

The MFT 3 occurrence of fossil assemblage having a normal marine tolerance, particularly the foraminifera, brachiopods, gastropods, algae, corals, bryozoans, and echinoderm, within the MFT 3 suggests warm, shallow-marine shelf settings [33]. Brachiopods are particularly common in Palaeozoic and Mesozoic limestone of shallow-marine origin, and they are largely benthic, sessile organisms [38]. These organisms tolerate a salinity range of brackish to

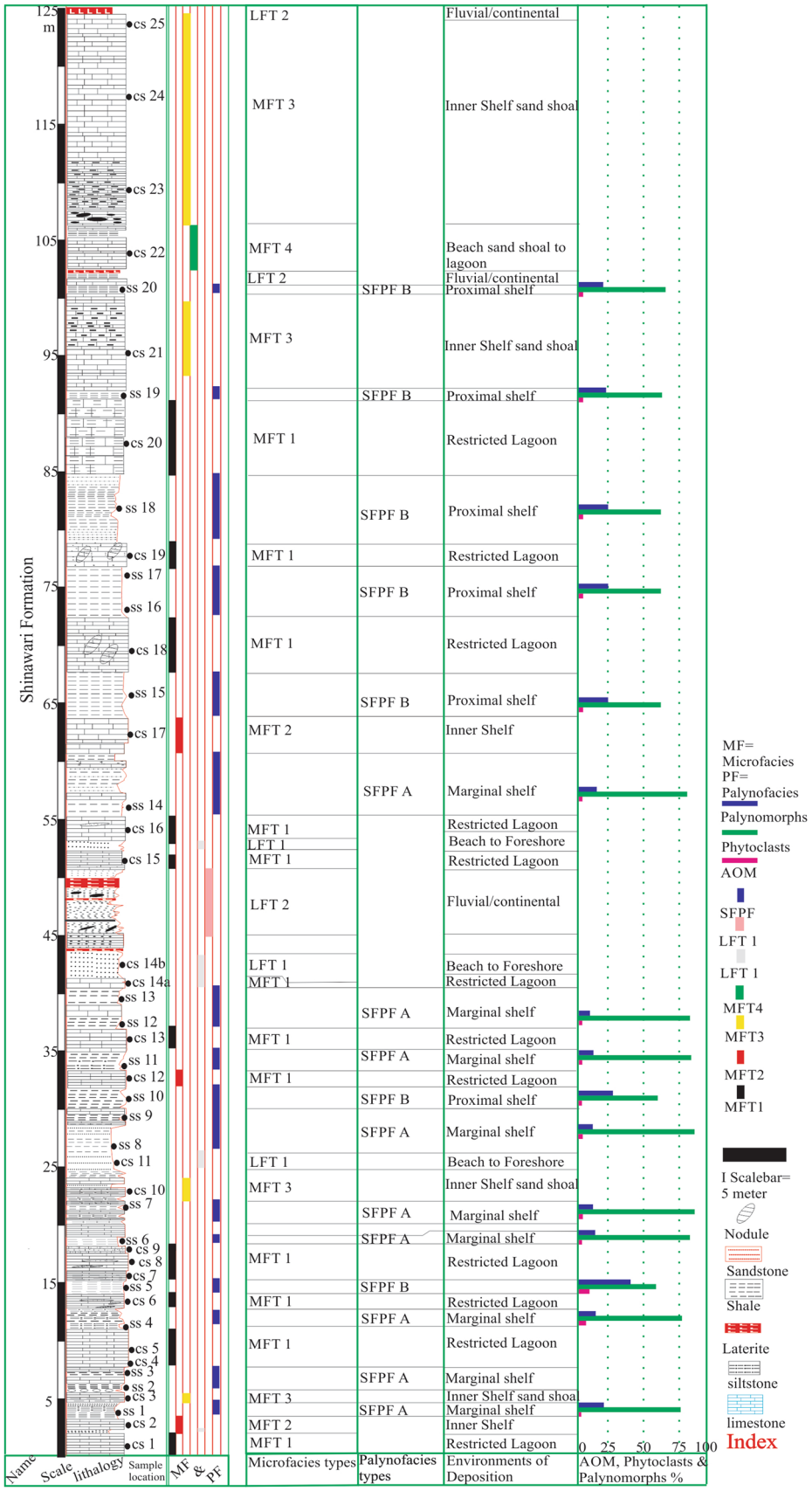

Fig. 3 Composite stratigraphic column of Shinawari Formation at Chichali Nala displaying relationship between microfacies and palynofacies (conti.....)

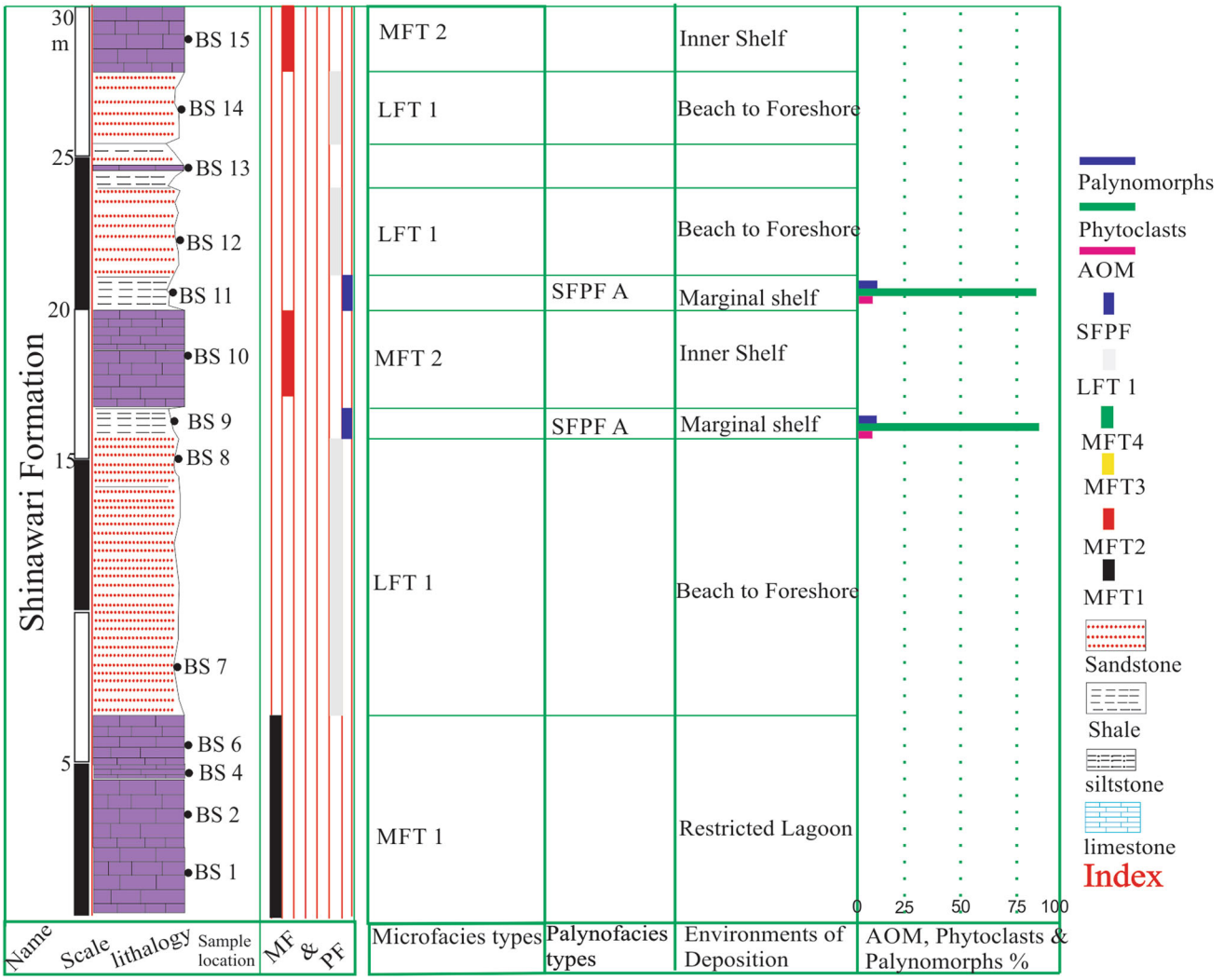

Fig. 4 Composite stratigraphic column of Shinawari Formation at Baroch Nala displaying relationship between microfacies and palynofacies (conti.....)

slightly hypersaline [33]. Bryozoans are small, colonial marine organisms that are significant suppliers of carbonate sediments [38]. Echinoderms are usually present in normal marine, open-shelf deposits [33]. Presence of cross-bedding on outcrops scale and grainstone textures shows a shallow environment showing oolitic or bioclastic shoal [39–41]. This microfacies correlates with the SMF-11 of Wilson [31] and Flugel [37,42] representing a shore line sand shoal to inner shelf settings with the intervention of high-energy conditions (Fig. 7).

3.1.4 Restricted Marine Shoals (MFT 4)

The MFT 4 is subdivided into two sub-facies MFT (A) and MFT (B).

The peloidal grainstone microfacies (MFT 4A) is represented by yellowish grey colour bedded limestone. The limestone is hard, compact, and micritic in nature (Fig. 2). The stratigraphic thickness and vertical distribution of MFT 4 microfacies are discussed in Table 1. The petrographic study reveals that, the microfacies is comprised of 55% peloids, 13% ooids, 10% quartz, 5% intraclasts, 1% brachiopod, and 1% echinoderms in a sparite. Quartz is medium to coarse grained with rounded outlines and is elongated to sub-spherical in shape. The peloids have variable dimension and geometric shapes representing polygenetic origin. In this microfacies, the recognizable skeletal allochems are echinoderms with other bioclasts (Figs. 3, 4, 5, 6, 9a, b).

The fossiliferous ooids–oncoids grainstone (MFT 4B) microfacies is represented by limestone of the cream colour, which is bedded. This microfacies is represented by sample GS 1 and is composed of 70% oncoids, 6% intraclasts with 5% echinoids, 5% brachiopods, 2% bivalves, and 2% algae. Oncoids are preserved without any internal modifi-

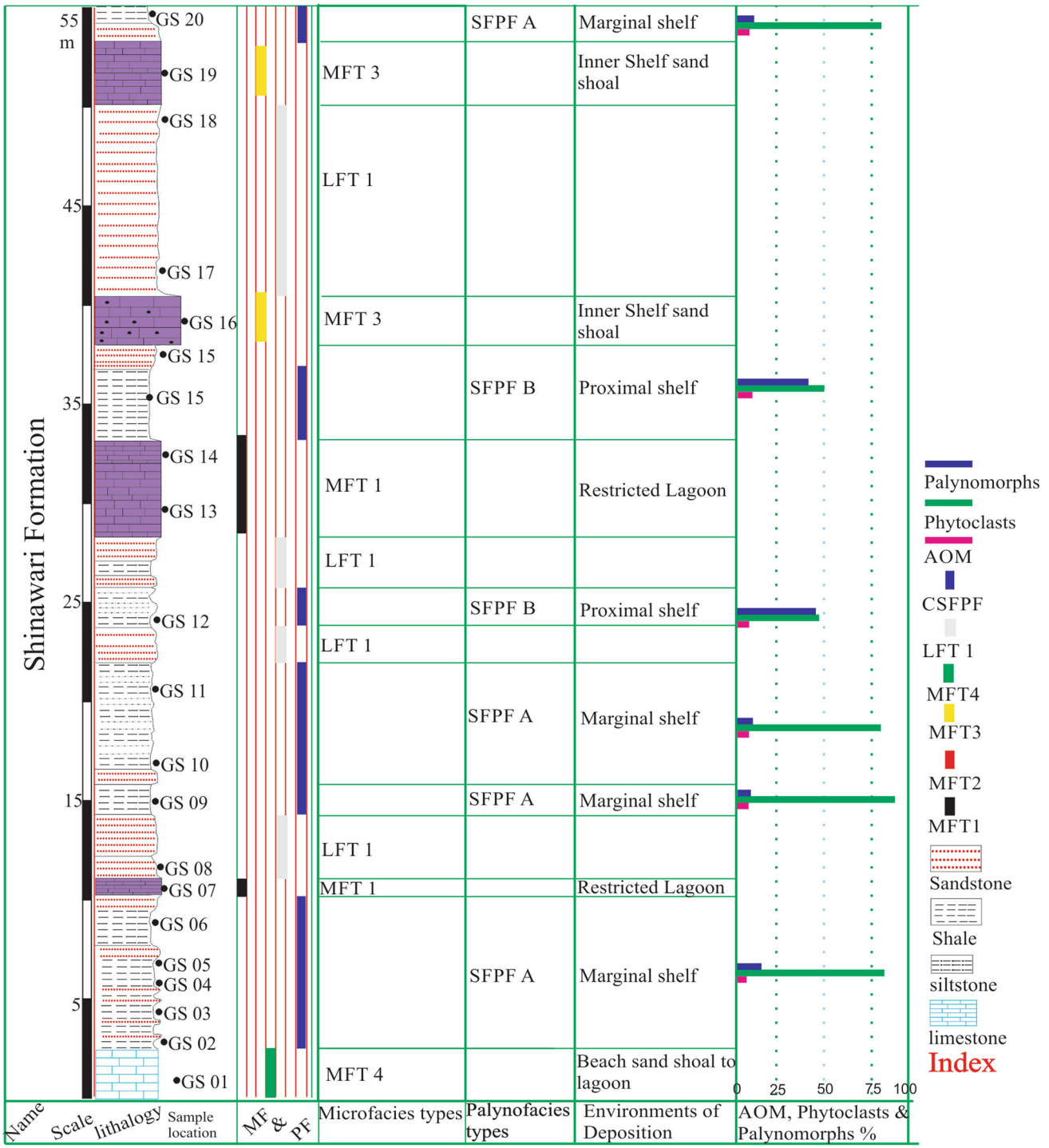

Fig. 5 Composite stratigraphic column of Shinawari Formation at Gula Khel Nala displaying relationship between microfacies and palynofacies (conti.....)

cation in the form of finely concentric tangential fabrics. The oncoids grains nuclei contain a variety of grains such as ooid, echinoderms, brachiopod, and gastropods. Some oncoids are perfectly spherical in shape, while some are elongated (Figs. 3, 4, 5, 6, 9c–f).

Interpretation

The MFT 4(A) is represented by skeletal and non-skeletal allochems. The non-skeletal allochems, i.e. peloids are found in protected, low-energy settings. The quartz grains in the facies appear to have been transported to the lagoon via

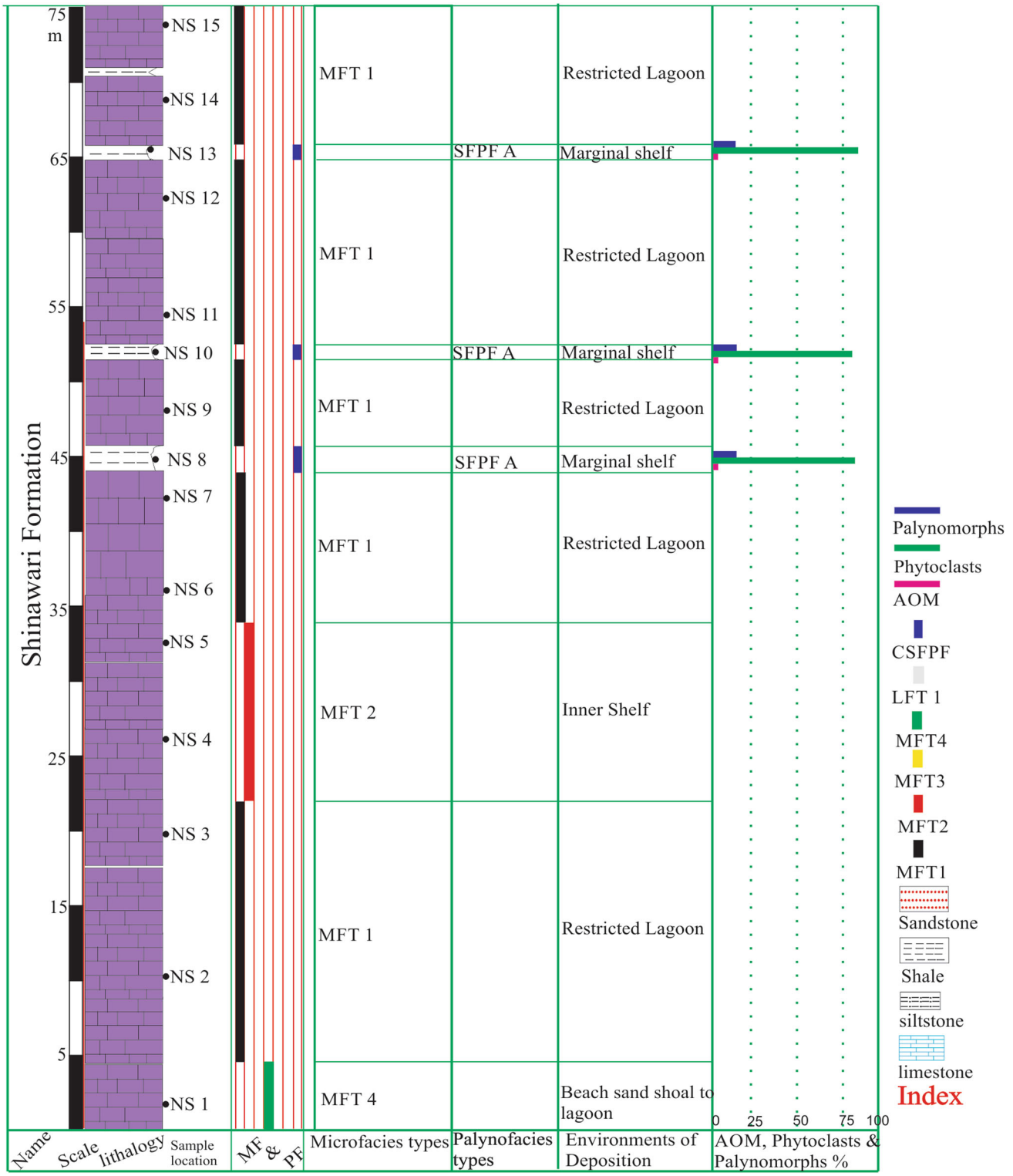

Fig. 6 Composite stratigraphic column of Shinawari Formation at Nizampur Section displaying relationship between microfacies and palynofacies

a nearby fluvial system and aeolian transport or reworking from the beach as a result of sea level fluctuations. The abundance of peloids within MFT 4(A) and scarcity of the skeletal allochems indicate restricted marine conditions of a lagoonal setting. However, the presence of other non-skeleton allochems like intraclasts and ooids suggests deposition in high-energy settings [34,35,43–48]. The peloid grainstone microfacies resembles the SMF-16 of Wilson

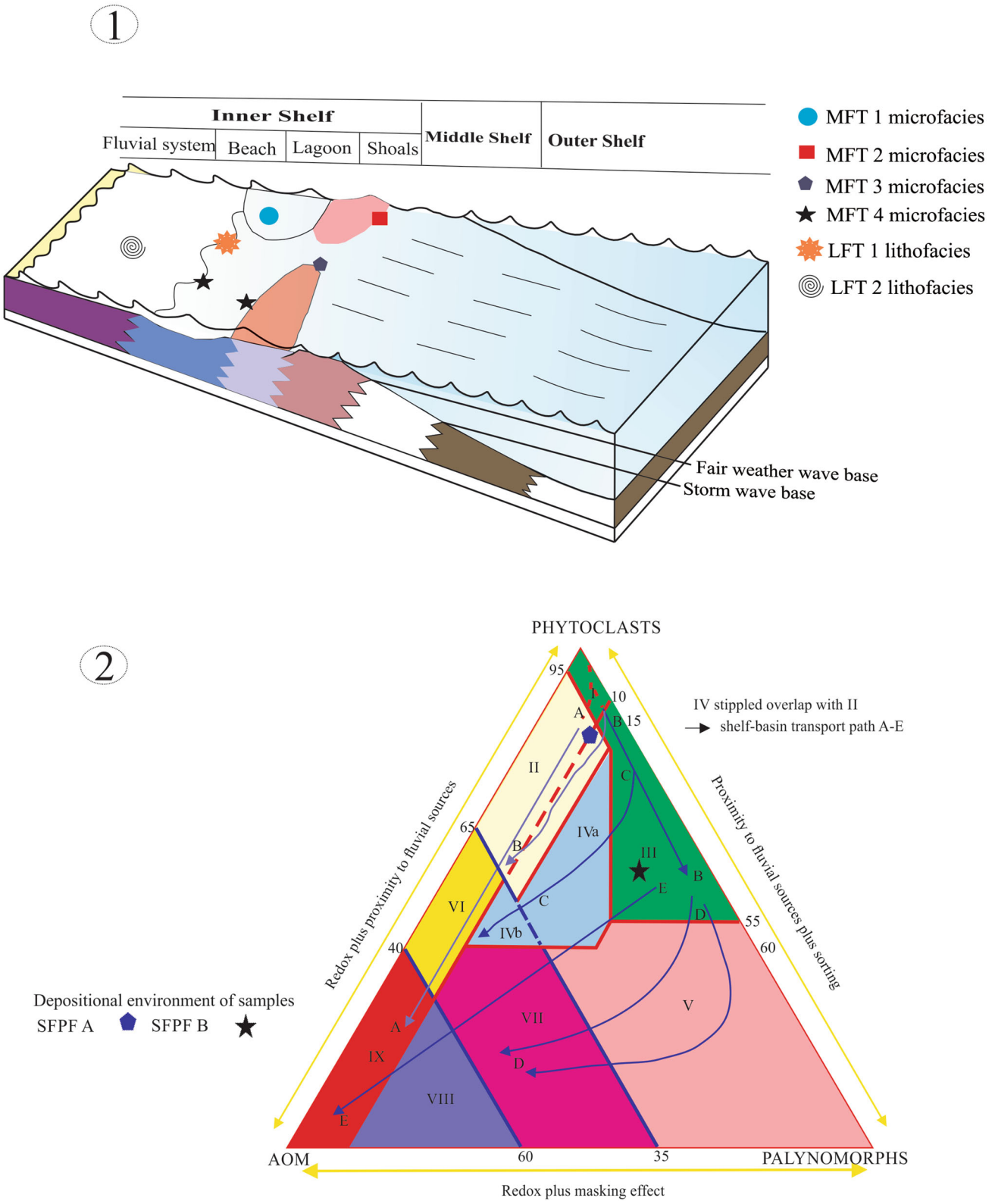

Fig. 7 Depositional model of Shinawari Formation in contexts of (1) microfacies and (2) ternary AOM–phytoclast–palynomorph kerogen plot showing depositional environments of palynofacies, i.e. SFPF-A and B (based on relative numeric frequency of organic matter)

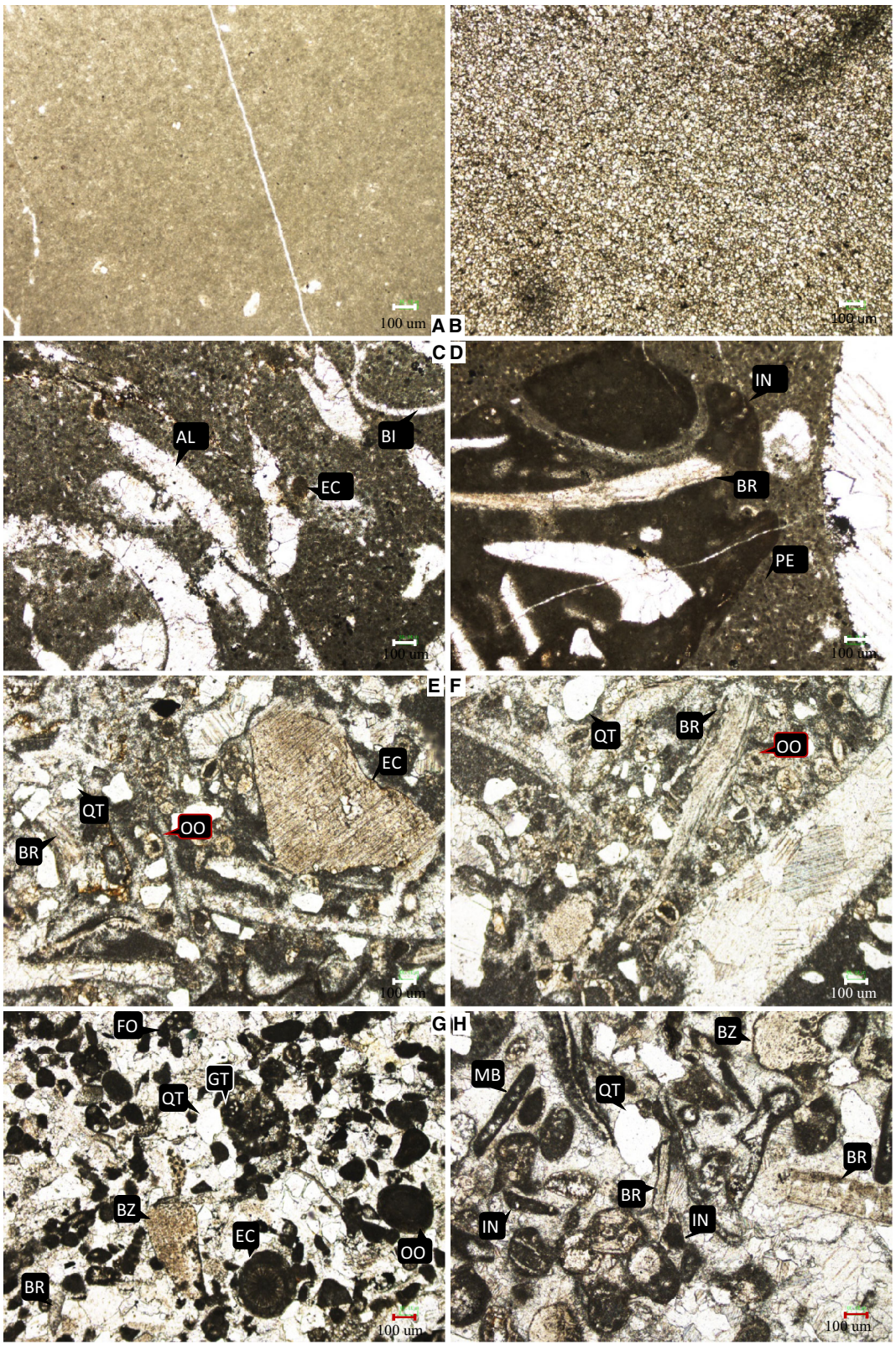

Fig. 8 Photomicrographs of **a** and **b** MFT 1(A) devoids of any allochems and dolomitization; **c** and **d** MFT 1(B) showing pellet (PE), bivalves (BI), intraclast (IN), brachiopods (BR), and echinoderm (EC); **e** and **f** describing MFT 2 presentation ooid (OO), echinoderms (EC), brachiopods (BR), and quartz (QT); **g** and **h** MFT 3 showing intraclast (IN), peloids (POL), brachiopods (BR), bryozoans (BZ), echinoderm (EC), foraminifera (FO), ooids (OO), micritized bioclasts (MB), and quartz extraclast (Qt)

[31], Brigaud et al. [41], and Flugel [36], representing sand shoal to a restricted lagoon (Fig. 7).

The MFT 4(B) Palaeozoic and Mesozoic oncoids are thought to be formed by cyanobacteria in shallow-marine setting [36,49]; furthermore, the coexistence of other marine fauna such as brachiopods, algae, and echinoderms supports shallow-marine interpretation [33,38]. This microfacies is correlated with the SMF-13 of Wilson [31], and Brigaud et al. [41] represent deposition in the peritidal to lagoon (Fig. 7).

3.1.5 For Shore Facies (LFT 1)

This facies is whitish, yellowish grey to dark grey thin to moderately bedded, burrowed, lenticular, planer to cross-laminated sandstone, and the lamination of cross-beds is planer in nature having a sharp angle with the planer surface. The sandstone is hard, fine to coarse grained, calcareous, and having no obvious trace fossils on its surface (Fig. 2 and Table 1). On the basis of microscopic studies, the lithofacies show skeletal bioclasts of algae (1%), brachiopods (1%), quartz (70%), feldspar (13%), mica (5%), and rock fragment (2%). The feldspar is present in the form of both alkali, plagioclase, and mica in the form of muscovite and biotite. The cementing material is calcareous. The quartz grains are dominantly monocrystalline with the minor amount of polycrystalline. The gains are moderately sorted, sub-rounded with planer to tangential contacts. The lithofacies is named as sub-arkose quartz arenites according to Folk [18] ternary sandstone classification scheme. With respect to stratigraphic thickness and vertical distribution, the LFT 1 data are presented in Table 1 (Figs. 3, 4, 5, 6, 9g, h).

Interpretation

The occurrence of planar, low-angle cross-beds represents foreshore (inner ramp/shelf) depositional environments, while the bioturbation (verticals and tubes shapes) represents deeper parts of the foreshore (shallow subtidal environments) [50–53]. Based on the presence of intraclasts, feldspar, and rounded and spherical quartz, this microfacies is assumed to be deposited in a foreshore (beach to foreshore) depositional setting (Fig. 7).

3.1.6 Fluvial/Continental Facies (LFT 2)

This lithofacies is composed of argillaceous sandstone, laterite, coal, and sandy limestone/marl. The different lithological units are in interbedded form. The sandstone is thin to medium bedded, fine to medium grained, reddish to white in colour, and soft and fragile in nature. Coal occurs in the form of thin seams and disseminated lenses. The low-grade coal seams are 0.1 metres thick, dull and black in colour, and not enough thick for commercial uses. Sulphur disseminations in form of pyrite are also associated with the coal seams. The laterite beds are present at different intervals within this lithofacies, which are thin bedded and reddish in colour (Figs. 3, 4, 5, 6 and Table 1).

Interpretation

The reddish to brownish colour of laterite is due to the unique optical behaviour of hematites (Fe_2O_3) [54]. This lithofacies often develops within the regressive phase of sea level fluctuation and sub-aerial exposure, which may indicate forms a major unconformity. The presence of laterite and limonite shows an oxidizing state, thus pointing to its formation in a continental geological setting above the groundwater table in non-marine systems [39,55–57]. So based on available information, we interpret the depositional setting as terrestrial/continental.

In this lithofacies, the coal is of dull black colour that represents accumulation under the anoxic condition in restricted marshy palaeoenvironmental settings. These marshes were dominated by a sandy fluvial depositional system with surface exposure of interfluvial areas resulting in the development of laterites (Fig. 7).

3.1.7 Discussion on Depositional Model

The integrated approach makes it possible to assess the depositional history which includes mixed lithologies of limestone, sandstone, and shale, with subordinate laterites, siltstone with few layers of coal layers. The depositional setting for various components has been addressed by microfacies analysis of limestone, palynofacies analysis of shale, and lithofacies analysis of sandstone units. The integrated approach makes it possible to assess the depositional history in detail, which includes a fluvial dominated, peritidal lagoon, beach shoal to distal shelf setting [1,31–57] and (Fig. 7). According to Ahmed et al. [9], the Shinawari Formation in the salt range is studied at different localities such as the Daud Khel and Thatti sections portray deposition setting ranging from coastal to open-marine environments at the time of deposition in the Middle Jurassic. The depositional history and stratigraphic thickness of same stratigraphic units in Upper Indus Basin are not the same in all its studied sections. The possible reason may be prevailing tectonic activates at the time of middle Jurassic [58].

The Jaisalmer Basin, India, which represents an eastward extension of the Indus Basin of Pakistan also contains the middle Jurassic Jaisalmer Formation which is considered time equivalent of the Shinawri Formation, Pakistan, and is comprised of a mixed clastic and carbonate units. The geological setting of the Jaisalmer Formation is dominantly marine in nature as deduced from the calcareous sandstone, shale/marls, mudstone, wackstone, oolitic grainstone, and oolitic–bioclastic grainstone microfacies [59–61]. The environment of deposition of Jaisalmer Formation is similar to the Shinawari Formation, suggesting that marine environment with high energy condition prevailed in middle Jurassic.

The time equivalent succession of Shinawari Formation in Qaidam Basin, Dameigou, north-western China, is represented by Dameigou and Caishiling formations. The strata comprising of mudstone, coal, and sandstone with conglomerate are interpreted to have been deposited in lacustrine, fluvial, and deltaic settings, respectively [62–66]. The geological features of the Jurassic stratigraphic units are mostly analogous to other basins in NW China and with nearby Junggar, Turpan-Hami, and Intra-Mongolia Basins [67]. From the regional correlation in eastern Tethys, the depositional spectrum of middle Jurassic is somewhat analogue with each other; otherwise, it does not seem perfect that the exact facies recorded in Indus Basin are also present in Qaidam Basin of China and its nearby basins.

4 Palynofacies and Hydrocarbon Source Rock Evaluation

4.1 Palynofacies

Palynofacies studies were undertaken to assess the palaeoenvironment and to evaluate whether the Shinawari Formation in this area is oil or gas prone. Two types of palynofacies are defined herein and denoted as SFPF-A and -B. The SFPF stands for Shinawari Formation palynofacies.

4.1.1 Palynofacies SFPF-A

Description

In this palynofacies, phytoclasts dominate (85–86%) of total particulate organic matter. The phytoclasts are mostly opaque and brownish in colour. Their shape varies from spherical to elongated and bladed. The palynomorphs (10%) constitute the second dominant organic matter of the total constituents, while amorphous organic matter (AOM) (5%) constitutes the third components of the palynofacies. The colour of AOM ranges from light grey to reddish in transmitted light. Palynofacies SFPF-A is comprised of mixed spherical, elongated to bladed phytoclasts; however, the elongated to bladed forms represent the dominant fraction among other palynofacies constituents. Examples of this palynofacies are shown in Figs. 3, 4, 5, 6, and 10a–c.

Interpretation

SFPF-A plots in the type II field on the Tyson [1] AOM–phytoclast–palynomorph ternary diagram corresponding to a marginal dysoxic–anoxic basinal setting are shown in Fig 7. The dominance of elongated to bladed phytoclasts in this palynofacies suggests the short duration of transportation from the terrestrial derived source [1], supporting the deposition of these palynofacies in marginal marine environments. In addition, the AOM in this palynofacies is the light grey to reddish brown colour. The minor occurrences of AOM suggest the scarcity of nutrients supply and/or high oxygen in the water column [1,68]. Such types of limited marine effects are typical of marginal marine settings, whereby the terrestrial processes dominate.

4.1.2 Palynofacies SFPF-B

Description

In palynofacies, SFPF-B phytoclasts are the most abundant and reaches 57% of the total constituents. These phytoclasts are opaque (black), while the non-opaque kind is reddish brown. These phytoclasts are internally structureless and show a verity of shapes such as elongated, circular/spherical, and bladed. The palynomorphs and the AOM make up about 33% and 10% of the total palynofacies constituents, respectively. The colour of AOM ranges from grey to yellowish grey. The typical distribution of this palynofacies is given in Figs. 3, 4, 5, 6, and 10d–f.

Interpretation

Palynofacies CSFPF-B falls within the Tyson [1] type III field, representing a heterolithic, proximal shelf depositional setting (Fig. 7).

4.2 Hydrocarbon Source Rock Evaluation

The organic matter with its sub-types and palaeoenvironmental condition are considered very significant for the evaluation of source rock potential [1,13–16,30]. The humic and sapropelic types of organic matter recognized in the studied Shinawari Formation are categorized as terrestrial and marine derived. The preserved spores and pollen are recognized to be rich in lipids, which mostly yield liquid hydrocarbons [69,70]. Spores and pollen (range 9–45%; average: 17%) are abundant in the Shinawari Formation ranges (Fig. 11c–s, 3–6). The phytoclasts abundance ranges from 56 to 57%. The translucent (non-opaque) or opaque (black) phytoclast is related to the kerogen type III (Fig. 11t–ee) comprising its major parts ranging from 48 to 89%. The structured terrestrial (wood/cuticle) organic matter and black debris/charcoal which has no or negligible source rock potentials are less than 1%. Structured marine (i.e. phytoplankton) organic matter is mainly contributed by dinoflagellates and foraminiferal linings (Fig. 11ff–hh), having a count frequency ranging from 0.1 to 0.5%. The frequency of amorphous organic matter, a good source of liquid hydrocarbons, is low (5–10%), and its average value is 10%, (Fig. 11ii–mm). The dominance of phytoclasts and spores/pollen, with subordinate amorphous organic matter and biodegraded terrestrial organic matter in the Shinawari Formation, indicates good quality kerogen, but the hydrocarbons source rock potential may be limited by the generally low TOC.

Spore colour index (SCI) and thermal alteration index (TAI) can be used to determine the maturity of potential

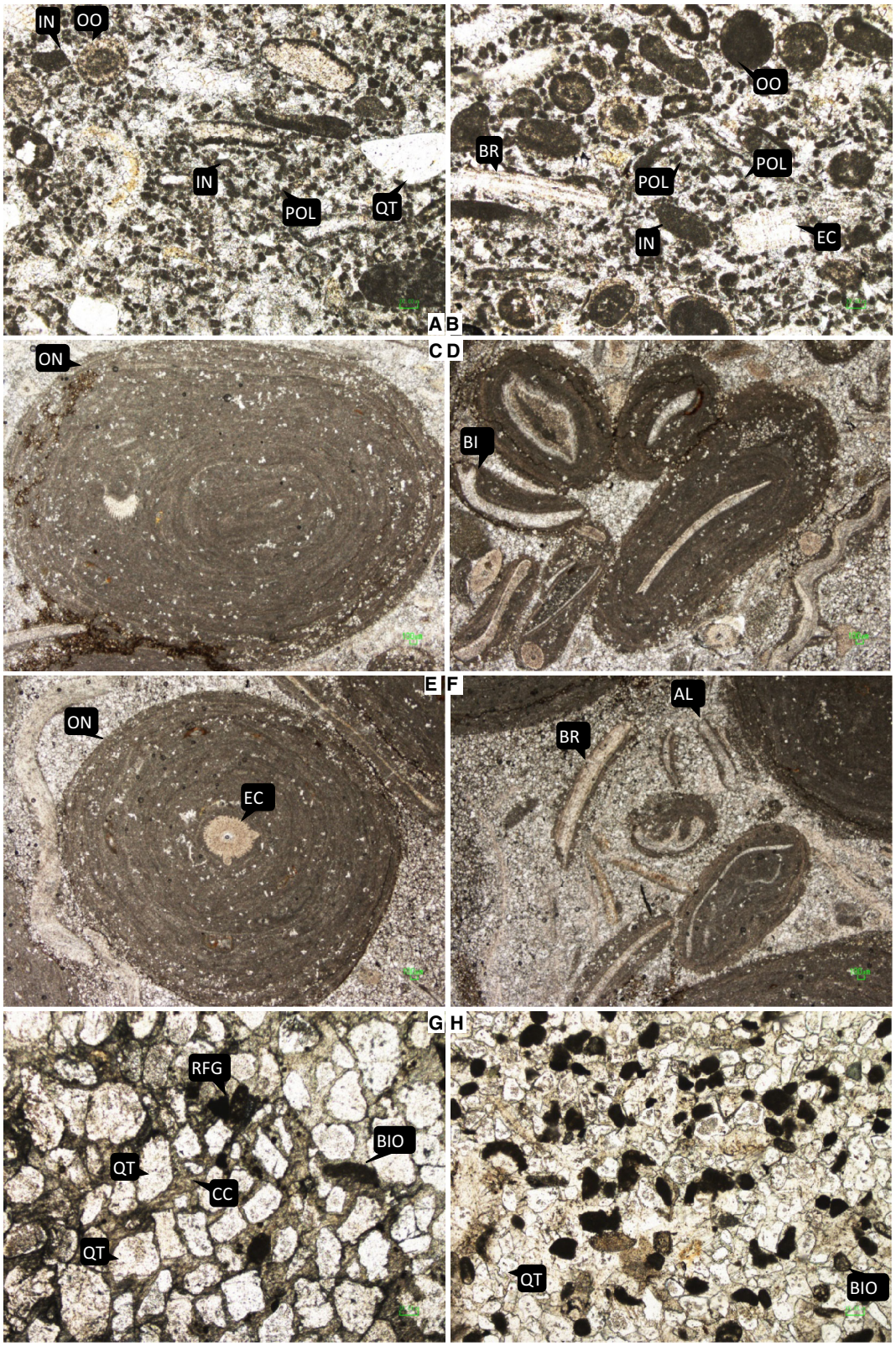

Fig. 9 Photomicrographs of **a** and **b** describing MFT 4(A) showing peloids (POL), quartz extraclasts (QT), intraclasts (IN), brachiopods (BR), and echinoderm (EC); **c–f** showing MFT 4(B) describing oncoids (ON), echinoderm (EC), bivalve (BI), brachiopods (BR), and algae (AL); **g** and **h** showing LFT 1 sub-arkose quartz arenite lithofacies displaying quartz extraclasts (QT) and rock fragments (RF), bioclasts (BIO) in calcareous cements (CC)

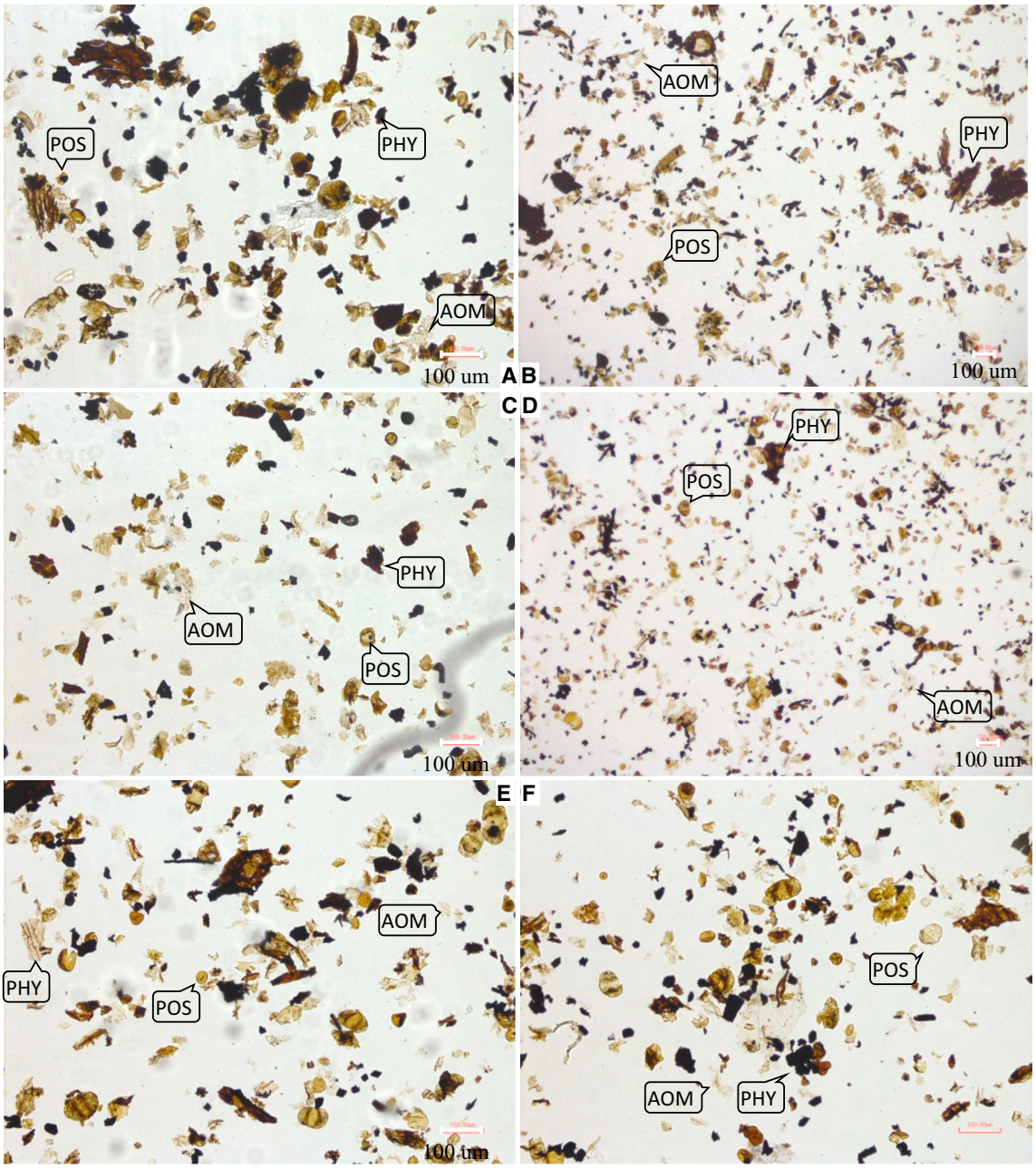

Fig. 10 Photomicrographs of **a**, **b** and **c** SFPF-A and **c**, **d**, and **e** SFPF-B; delineating phytoclasts (PHY), pollen/spore (POS), and amorphous organic matter (AOM). Furthermore, **g** and **h** mudstone microfacies

source rocks [71]. The spore colour index (SCI) ranges from 1 to 10 and reflects colourless to pale yellow to black colouration [28]. This colour change is due to progressive variation in the temperature, burial depth, and time and is also being expressed as the thermal alteration index (TAI). The TAI can easily be determined from the colour of pollen and spores under a simple polarizing microscope and also by using the translucency of organic matter from photoelectric measurements. The TAI is assessed from the colour of spore and pollen before the oxidation treatment of the samples and by using five-point scales of Staplin [26,27] and Utting and Hamblin [28]. Shale outcrops samples were studied from all studies sections, and the colour of each spore and pollen was investigated and compared with the standard SCI and TAI. The particular value was assigned to every sample by taking the average colour of spore and pollen, and SCI ranged from 5 to 7, which is in the main oil and wet gas window. The TAI was measured as 2 to 3+ and is also in the main oil and gas generation window (Fig. 12).

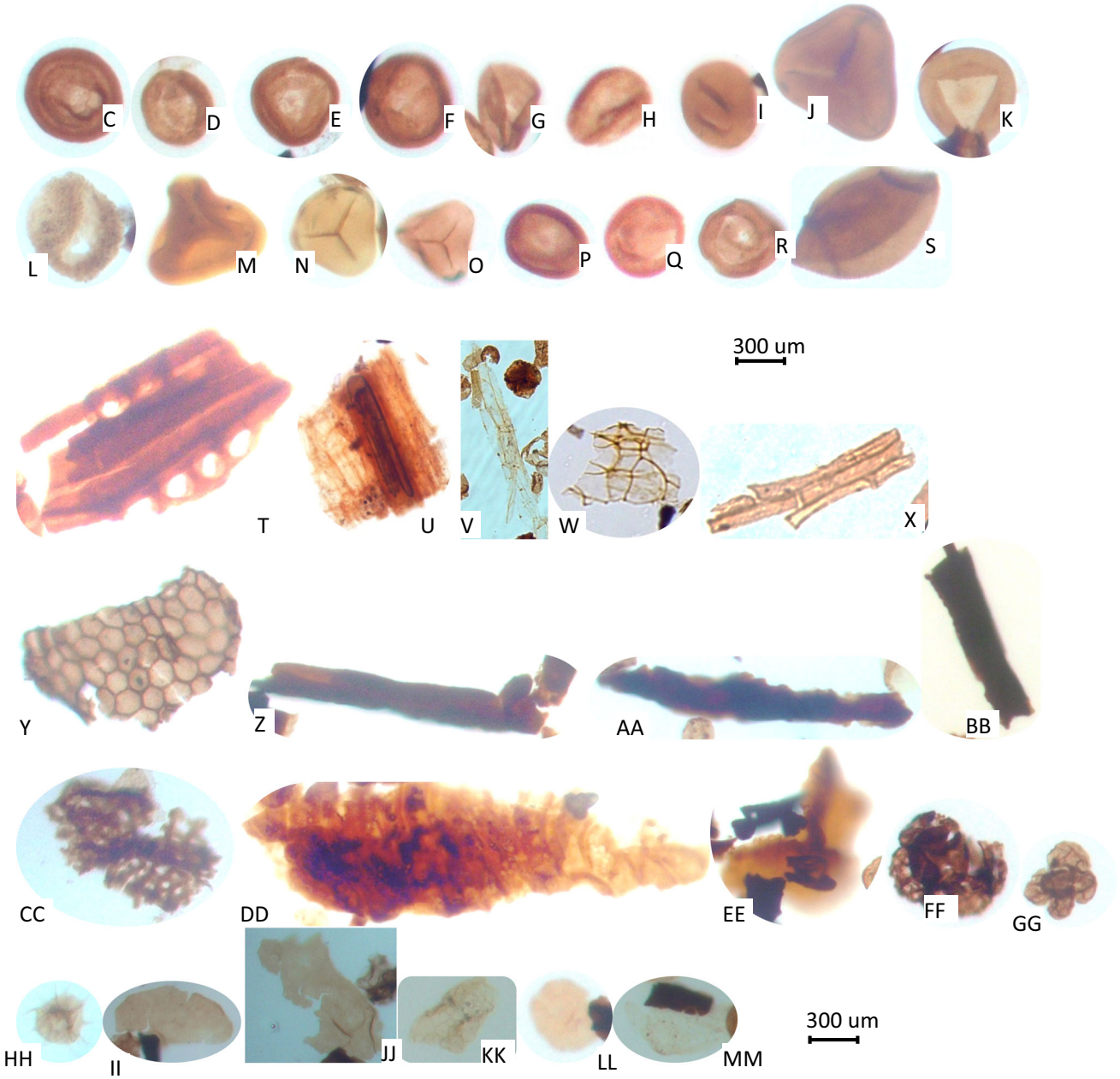

Fig. 11 **c–s** Pollen and spore; **t–ee** phytoclast group; **ff–hh** structured marine (phytoplankton); and **ii–mm** amorphous organic matter

Palynofacies components include phytoclasts, palynomorphs, and amorphous organic matter (AOM) and can also be classified as macerals for kerogen classification. As described by various workers, we have assigned vitrinite to brown phytoclasts, inertinite for black phytoclasts, and cutinite for light brown or yellow phytoclasts [68,72,73]. Opaque/black phytoclasts are responsible for the dry gas generation and are categorized as kerogen type IV. The translucent/brown phytoclasts are responsible for both oil and gas on thermal maturation and categorized as kerogen type III [69,74]. Moreover, pollen and spores are rich in lipids, mostly representing the kerogen type II, which contribute to the liquid hydrocarbons [69,70]. According to Ercegovac and Kostić [68], the terms alginite and liptinite are used for palynomorphs are used, categorized as kerogen type I. Most fossilized marine organic matter is represented by amorphous organic matter (AOM) and is prone to oil generation on thermal maturation categorized as kerogen type I; AOM may be marine or non-marine. The liptinite–vitrinite–inertinite (LVI) kerogen plots of Dow and O'Connor [22] were used for kerogen classification (Fig. 13) and to indicate the hydrocarbons that may be generated from these kerogens (i.e. oil and gas

Palynofacies types	Spore Color Index	Thermal Alteration Index	Specimen Photomicrographs
SFPF B Proximal shelf	7	3	
	5	2	
	6	-3	
	7	3	
SFPF A Marginal shelf	8	+3	
	5	+3	
	7	3	
SFPF B Proximal shelf	5	2	
SFPF A Marginal shelf	8	+3	
	7	3	

Fig. 12 Values of spore colour index (SCI) and thermal alteration index (TAI) from photomicrographs of palynomorphs

both dry gas and wet gas). Using the LVI ternary kerogen plots of Dow and O'Connor [22], the SFPF-A characterized by 15% brown phytoclasts, 70% black phytoclasts, 5% AOM, and 10% palynomorphs lies in the domain of kerogen type III or IV, which could be a source of the dry gas or barren field. The CSFPF-B having 7% brown phytoclasts, 58% black phytoclasts, 10% AOM, and 33% palynomorphs lies in the domain of kerogen type II favourable for both oil and gas generation on the thermal maturation (Fig. 13).

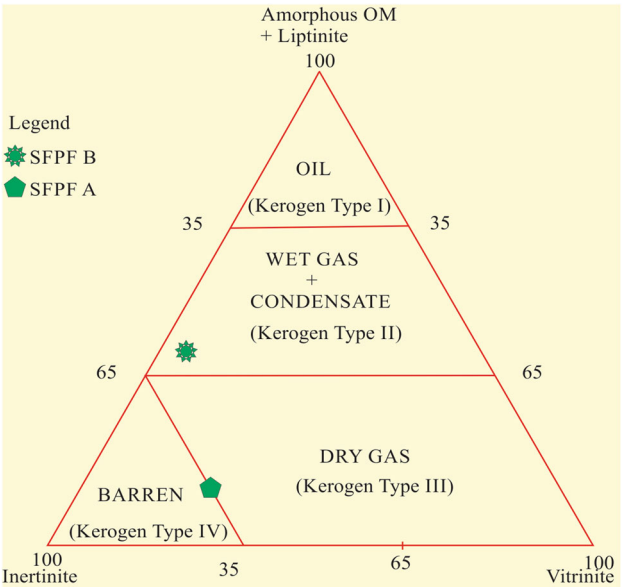

Fig. 13 Liptinite–vitrinite–inertinite (LVI) ternary kerogen plot with legend indicating kerogen types

5 Geochemical Methods

The geochemical analysis such as total organic carbon (TOC) and Rock-Eval pyrolysis is frequently used to evaluate the organic-rich clastic or non-clastic source rock. These geochemical-based techniques are prompt and economical.

The quantity and quality of source rock can be evaluated by the total organic carbon (TOC) and Rock-Eval pyrolysis data. Among the parameters generated from Rock-Eval are S1, a measure of the free (i.e. already generated) hydrocarbons, S2, a measure of the remaining generating potential, and S3 [29,75,76]. Table 2 shows the total organic carbon (TOC) content of the Shinawari Formation ranging from 0.17 to 2.09%, reflecting a poor to good source rock richness (Tab. 2). The TOC versus S2 cross-plot (Fig. 14a) shows poor–good generative potential, while S1 versus TOC

Table 2 Distribution of TOC and Rock-Eval data in different sections of Upper Indus Basin, Pakistan

Samples	TOC (%)	S1 (mg/g)	S2 (mg/g)	S3 (mg/g)	T-max °C	G.P (S1 + S2)	PI (S1/S1 + S2)	HI (S2/TOC)	OI (S3/TOC)
Nizampur Section									
NS 10	0.17	0.04	0.06	0.58	366	0.1	1.06	0.35	3.41
NS 8	0.14	0.05	0.07	0.59	362	0.12	1.07	0.50	4.21
Chichali Nala									
SS 20	0.5	0.06	0.07	0.33	440	0.13	1.07	0.14	0.66
SS 19	0.5	0.09	0.09	0.31	440	0.18	1.09	0.18	0.62
SS 18	0.7	0.44	1.03	1.23	437	1.47	2.03	1.47	1.76
SS 17	0.4	0.11	0.25	0.55	330	0.36	1.25	0.63	1.38
SS 16	0.5	0.51	0.3	0.9	441	0.81	1.3	0.60	1.80
SS 15	0.5	0.65	0.5	0.8	440	1.15	1.5	1.00	1.60
SS 14	0.2	0.01	0.02	0.11	444	0.03	1.02	0.10	0.55
SS 13	1.5	0.32	0.5	0.7	435	0.82	1.5	0.33	0.47
SS 12	0.8	0.3	0.7	0.13	455	1	1.7	0.88	0.16
SS 11	0.4	0.08	0.25	0.45	335	0.33	1.25	0.63	1.13
SS 10	0.5	0.16	1.01	0.03	427	1.17	2.01	2.02	0.06
SS 9	1.36	0.17	0.85	0.62	431	1.02	1.85	0.63	0.46
SS 8	0.5	0.41	0.8	0.6	435	1.21	1.8	1.60	1.20
SS 7	0.5	0.14	0.11	0.33	439	0.25	1.11	0.22	0.66
SS 6	0.5	0.04	0.08	0.43	442	0.12	1.08	0.16	0.86
SS 5	0.2	0.04	0.03	0.23	435	0.07	1.03	0.15	1.15
SS 4	0.4	0.1	0.24	0.65	325	0.34	1.24	0.60	1.63
SS 3	0.2	0	0	0.25	320	0	0	0.00	1.25
SS 2	0.5	0.6	0.9	0.5	430	1.5	1.9	1.80	1.00
SS 1	0.5	0.5	0.7	0.6	433	1.2	1.7	1.40	1.20
Baroch Nala									
BS 13	0.62	0.12	0.35	0.31	447	0.47	1.35	0.56	0.50
BS 11	1.37	0.11	0.23	0.97	432	0.34	1.23	0.17	0.71
BS 9	0.51	0.02	0.05	0.42	421	0.07	1.05	0.10	0.82
Gula Khel Nala									
GS 20	0.62	0.02	0.23	0.13	431	0.25	1.23	0.37	0.21
GS 15	0.56	0.2	0.6	0.6	431	0.8	1.6	1.07	1.07
GS 12	0.61	0.02	0.23	0.13	432	0.25	0	0.38	0.21
GS 10	1.05	0.14	4.42	0.35	448	4.56	5.42	4.21	0.33
GS 9	0.78	0.02	0.23	0.13	445	0.25	1.23	0.29	0.17
GS 6	2.09	1.45	23.75	13.03	429	25.2	24.75	11.36	6.23
GS 5	1.07	0.89	4.45	0.78	445	5.34	5.45	4.16	0.73
GS 4	0.71	0.44	0.98	1.01	437	1.42	1.98	1.38	1.42
GS 3	0.98	0.41	0.88	1.09	440	1.29	1.88	0.90	1.11
GS 2	0.5	0.04	0.08	0.45	431	0.12	1.08	0.16	0.90

(Fig. 14b) suggests the residual hydrocarbons are indigenous [77–79].

Pyrolysis analysis can also be used to quantify generation potential (GP) of a source rock expressed as the sum of values S1 and S2 expressed in equivalent units of kg/ton, and the quality of the source rock expressed as the Hydrogen Index (HI), which is a derivative of S2 and TOC. Source rocks with GPI < 2 are generally considered poor, while GP ranges from 2 to 5, from 5 to 10, and > 10 are considered to have fair, good, and very good, respectively [80]. Our GP of 0.8 to 1.2 indicates that the analysed intervals are not prolific hydrocarbon producers, and samples values more than 2 are hydrocarbon potentials (Table 2), which is generally

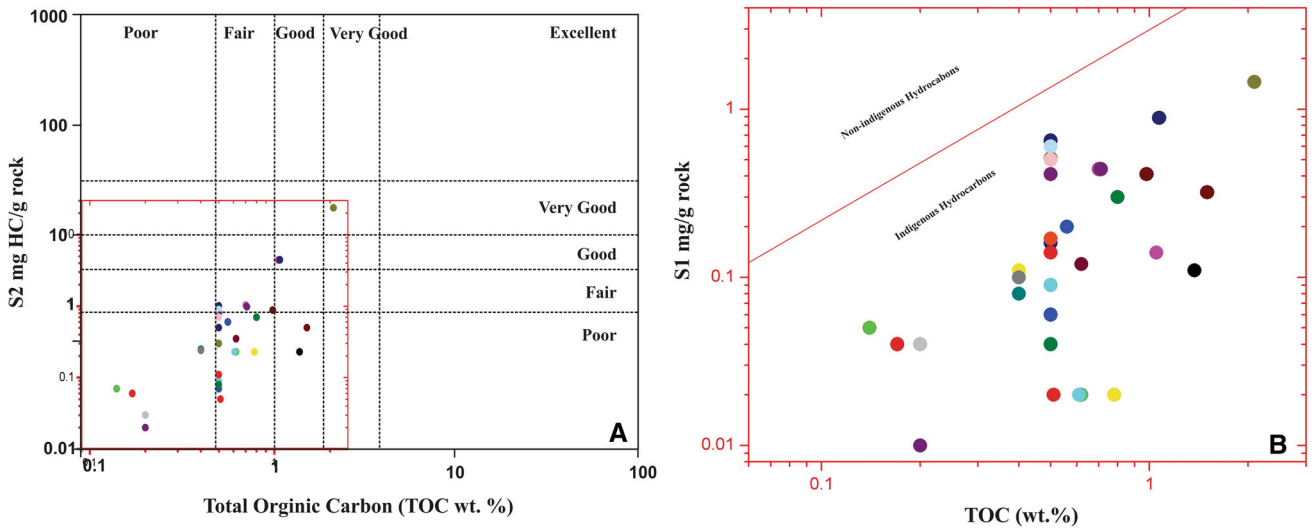

Fig. 14 Quality and quantity of organic matter of Jurassic source rocks, Surghar Range area, Punjab, Pakistan

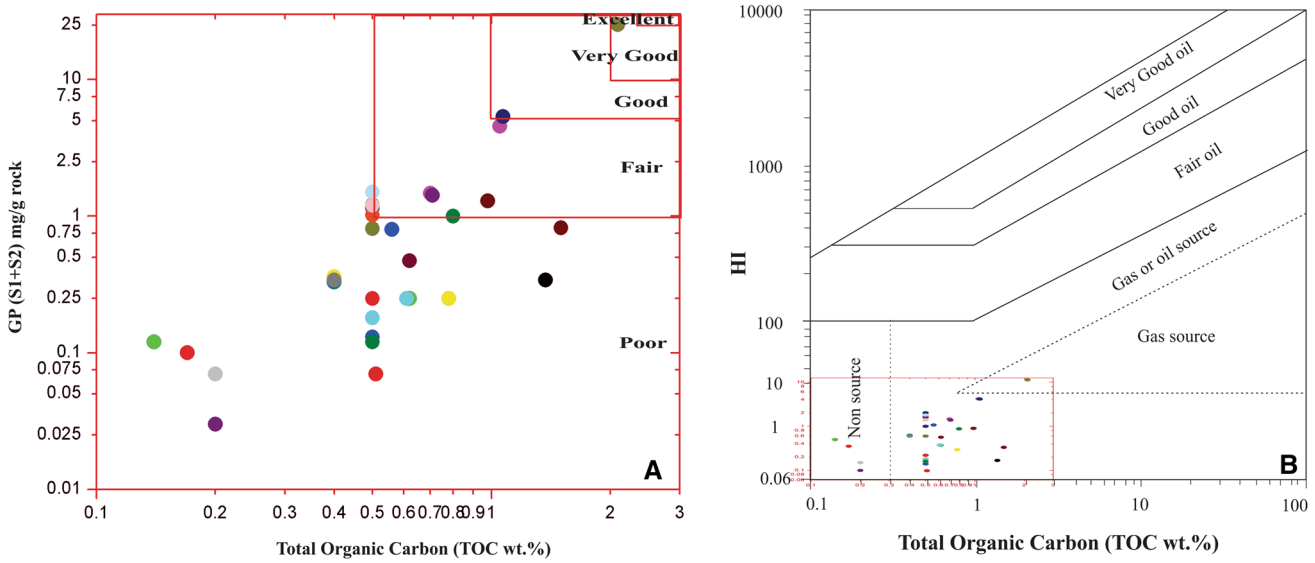

Fig. 15 Generation potential of organic matter of Jurassic source rocks, Surghar Range area, Punjab, Pakistan

confirmed by the cross-plot of the TOC and GP (Fig. 15a) [81]. The TOC versus HI cross-plot is shown in Fig. 15b.

The early genetic type of organic contents of a specific source rock is vital for the estimation of oil and gas potential. According to Waples [81], HI can be used to distinguish among the sub-types of kerogen. The HI value less than < 150 mg/g shows a possible source for producing gas from mainly kerogen type III, while the HI ranges between 150 and 300 mg/g having kerogen type III are adept in producing mixed oil and gas but chiefly gas generation. Rocks having HI value more than > 300 contain a substantial amount of type II (marine) kerogen which is capable of producing good oil and minor gas. The rocks with HI value more than > 600 frequently consist of almost type I or II (lacustrine) kerogen, which has exceptional potential to produce oil. In order to more precisely determine kerogen types for this investigation, the Krevelen classification scheme [23] was used to plot HI versus OI values (Fig. 16a) Bordenove et al. [24] and Langford and Blanc-Valleron classification scheme [25] was used to plot TOC versus S2 values (Fig. 16b, Table 2). These plots suggest that both types III and mixed type II/III kerogen are present in our Shinawari Formation samples.

Organic-rich source rock produces hydrocarbons when subjected to the geothermal gradient during its burial history [76]. The total amount and distribution of hydrocarbons produced depend on the types of organic matter, the extent of thermal alteration, and grading of thermal maturity [25,76]. The Rock-Eval pyrolysis temperature at maximum hydro-

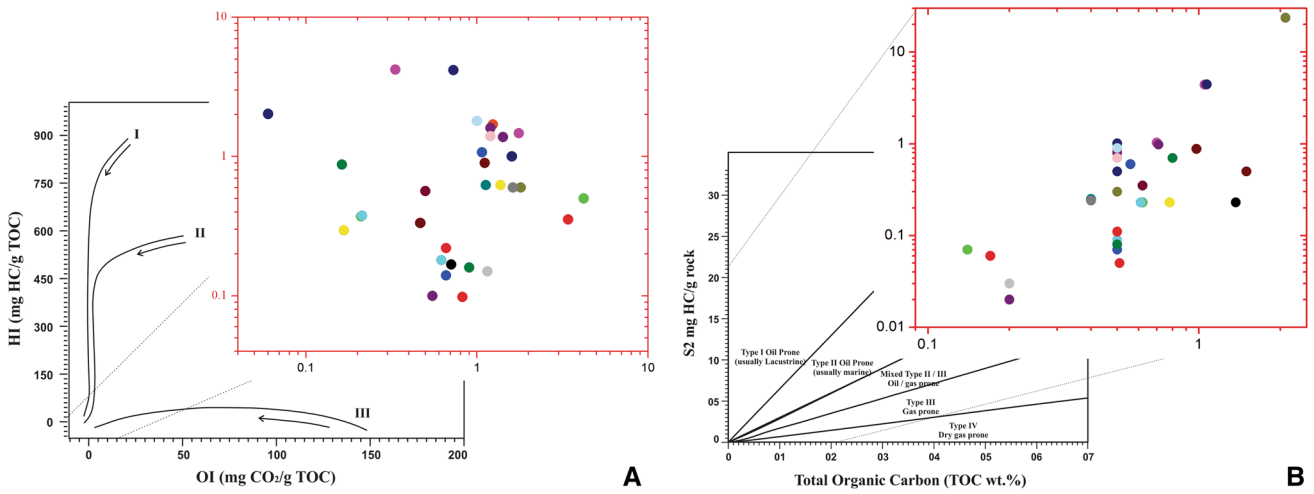

Fig. 16 Genetic type of organic matter of Jurassic source rocks, Surghar Range area, Punjab, Pakistan

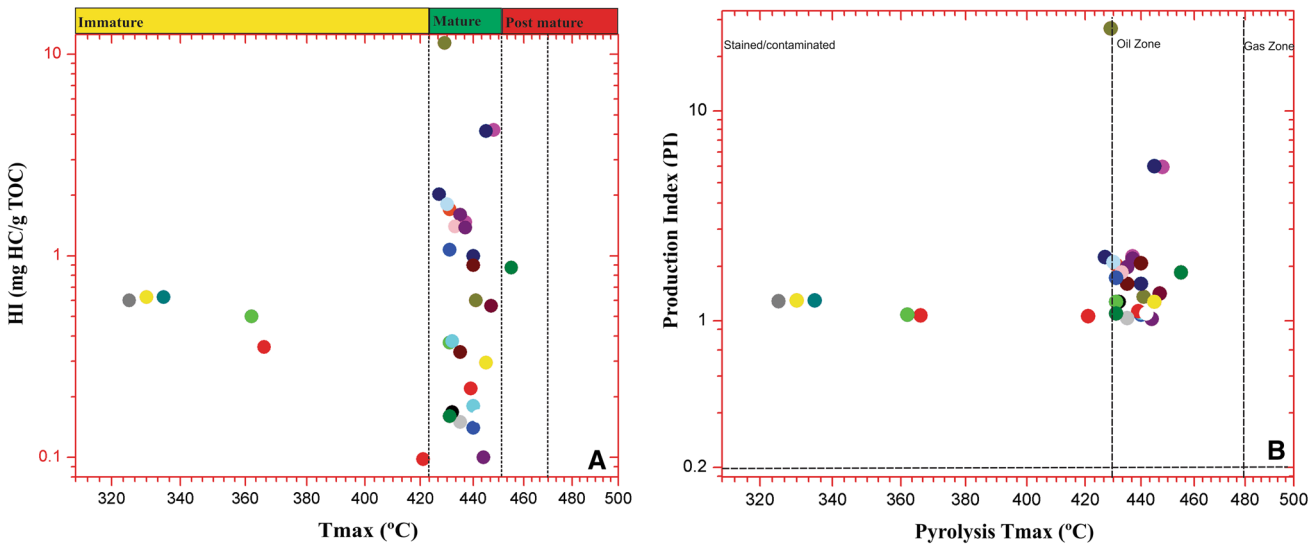

Fig. 17 Thermal maturation of organic matter of Jurassic source rocks, Surghar Range area, Punjab, Pakistan

carbon generation for the samples (Tmax) and production index (PI: the ratio of free to generated hydrocarbons, i.e. S1/S1 + S2) is used to find out the extent of thermal maturity [80,82]. The minimum temperature and production index required for oil generation begin at Tmax ranges between 435 and 465 °C and PI ranges between 0.2 and 0.4, while gas production starts at a "Tmax" of 470 °C and PI greater than 0.4 [75,82]. The kerogen types and maturity can be determined by using the value of HI versus Tmax cross-plot [82]. The HI versus Tmax plot (Fig 17a) and Tmax versus PI plot (Fig 17b and Table 2) of the samples of the Shinawri Formation demonstrate the presence of the type III kerogen, and a mature source rock nature [75,81], which is capable of generating oil.

The vitrinite reflectance is expressed by Ro(%), used to determine the thermal maturity of rocks. The vitrinite is a maceral which is an important component of the organic-rich shale and coal-derived from cellulose and lignin plant cell wall. The number of Ro(%) changes with the thermal maturity which is used to demarcate the oil and gas boundaries [76,83,84]. The vitrinite reflectance (VR) of the studied samples ranging from Ro(%) = 1.16 to 1.22 lies in oil to wet gas zone.

6 Conclusions

As a result of this research, the following conclusions have been drawn:

1. The Shinawari Formation in the Upper Indus Basin is moderate to the thick sequence of carbonate and clastic sediments of middle Jurassic age.

2. The stratigraphic micro- and lithofacies variation corroborated with the palynofacies information revealed deposition of the Shinawari Formation, i.e. peritidal lagoon, beach shoal to distal shelf setting.
3. The middle Jurassic of Upper Indus Basin is correlated with the India Indus Basin and China Qaidam Basin portraying somewhat same depositional setting.
4. The integration of palynofacies data, thermal alteration index (TAI), spore colour index, and vitrinite reflectance with organic geochemical analysis is used for source rock potentials.
5. The integrated approach of geochemical investigation indicates that kerogen type III and mixed type III/II are in the Tmax(°C) and VR of oil generation potentials.

Acknowledgements We acknowledge the support of the Bacha Khan University Charsadda, National Centre of Excellence in Geology (NCEG), University of Peshawar, Pakistan, and China University of Petroleum, East China (UPC). This project benefited from the Grant of China National Key Scientific Project (2016ZX05006-007) awarded to UPC and NCEG Project (PSF/Res/KPK/PU/Earth (96)). Furthermore, we gratefully acknowledge the efforts of Maqsood Ur Rehman, Tanveer Ahmad, and Tariq Mehmood (Department of Geology, Bacha Khan University Charsadda, Pakistan) during geological fieldwork.

References

1. Tyson, R.V.: Abundance of organic matter in sediments: TOC, hydrodynamic equivalence, dilution and flux effects. In: Tyson, R.V. (ed.) Sedimentary Organic Matter, pp. 81–118. Springer, Berlin (1995)
2. Fatmi, A.N.: Lithostratigraphic units of the Kohat-Potwar province, Upper Indus basin, Pakistan. Pak. Geol. Surv. Mem. **10**, 1–80 (1974)
3. Wandrey, C.J.; Law, B.; Shah, H.A.: Patala-Nammal Composite Total Petroleum System, Kohat-Potwar Geologic Province, Pakistan. US Department of the Interior, US Geological Survey, Reston (2004)
4. Kadri, I.: Petroleum Geology of Pakistan: Pakistan Petroleum Limited Karachi, Pakistan (1995)
5. Shah, M.I.: Stratigraphy of Pakistan, vol. 22 (Memories of Geological Survey of Pakistan; Ministry of Petroleum and Natural Resources of Geological Survey of Pakistan) (2009)
6. Danilchik, W.; Shah, S.: Stratigraphic nomenclature of formations in TransIndus Mountains Mianwali District, West Pakistan. US. Geology Survey, Project Report, pp. 1–45 (1967)
7. Fatmi, A.; Hyderi, I.; Anwar, M.: Occurrence of the Lower Jurassic Ammonoid genus Bouleiceras from the surghar range with a revised nomenclature of the Mesozoic Rocks of the Salt Range and Trans Indus Ranges (Upper Indus Basin). Geol. Bull. Punjab Univ. **25**, 38–46 (1990)
8. Fatmi, A.N.: Stratigraphy of the Jurassic and Lower Cretaceous rocks and Jurassic ammonites from northern areas of West Pakistan. British Museum (Natural History) (1972)
9. Ahmed, S.; Mertmann, D.; Manutsoglu, E.: Jurassic shelf sedimentation and sequence stratigraphy of the Surghar Range, Pakistan. J. Nepal Geol. Soc. **15**, 15–22 (1997)
10. Mertmann, D.; Ahmad, S.: Shinawari and Samana Suk Formations of the Surghar and salt ranges, Pakistan: facies and depositional environments. Z. Dtsch. Geol. Ges. **145**, 305–317 (1994)
11. Ali, F.; Ahmad, S.; Khan, S.; Hanif, M.; Qiang, J.: Toarcian–Bathonian palynostratigraphy and anoxic event in Pakistan: an organic geochemical study. Stratigraphy **15**(3), 225–243 (2018)
12. Batten, D.: Use of palynologic assemblage-types in Wealden correlation. Palaeontology **16**(1), 1–40 (1973)
13. Mendonça Filho, J.: Aplicação de estudos de palinofácies e fácies orgânica em rochas do Paleozóico da Bacia do Paraná, Sul do Brasil. Tese de Doutorado, Universidade Federal do Rio Grande do Sul, Santa Catarina, 2 vols (1999)
14. Mendonça Filho, J.; Carvalho, M.; Menezes, T.; Dutra, T.: Palinofácies. Técnicas e procedimentos para o trabalho com fósseis e formas modernas comparativas, vol. 1 (2002)
15. Mendonça Filho, J.; Menezes, T.; Mendonça, J.: Organic composition (palynofacies analysis). ICCP Training Course on Dispersed Organic Matter, pp. 33–81 (2011)
16. Silva, R.L.; Mendonça Filho, J.G.; Azerêdo, A.C.; Duarte, L.V.: Palynofacies and TOC analysis of marine and non-marine sediments across the Middle–Upper Jurassic boundary in the central-northern Lusitanian Basin (Portugal). Facies **60**(1), 255–276 (2014)
17. Dunham, R.J.: Classification of carbonate rocks according to depositional textures, pp. 108–121 (1962)
18. Folk, R.L.: Petrology of Sedimentary Rocks. Hemphill Publishing Company, Austin (1980)
19. Wood, G.; Gabriel, A.; Lawson, J.: Palynological techniques—processing and microscopy. In: Jansonius, J., McGregor, D.C. (eds.) Palynology: Principles and Applications, vol. 1, pp. 29–50. American Association of Stratigraphic Palynologists, Dallas (1996)
20. Steffen, D.; Gorin, G.: Palynofacies of the Upper Tithonian–Berriasian deep-sea carbonates in the Vocontian Trough (SE France). Bull Cent Rech Explor Prod Elf-Aquitaine **17**, 235–247 (1993)
21. Khan, S.: Biostratigraphy and microfacies of the cretaceous sediments in the Indus Basin, Pakistan (2013)
22. Dow, W.G.; O'Connor, D.I.: Kerogen Maturity and Type by Reflected Light Microscopy Applied to Petroleum Exploration. SEPM, Special Publication. SEPM, Broken Arrow (1982)
23. Krevelen, D.W.: Coal-Typology, Chemistry, Physics, Constitution, vol. 3. Elsevier, Amsterdam (1961)
24. Bordenove, M.L.; Espitalie, J.; Leplat, P.; Oudin, J.L.; Vandenbrouke, M.: Screening techniques for source rock evaluation. In: Bordenave, M.L. (ed.) Applied Petroleum Geochemistry, pp. 217–278. Technip & Ophrys Editions, Paris (1993)
25. Langford, F.; Blanc-Valleron, M.-M.: Interpreting Rock-Eval pyrolysis data using graphs of pyrolizable hydrocarbons vs. total organic carbon (1). AAPG Bull. **74**(6), 799–804 (1990)
26. Staplin, F.: Interpretation of thermal history from color of particulate organic matter—a review. Palynology **1**(1), 9–18 (1977)
27. Staplin, F.L.: Sedimentary organic matter, organic metamorphism, and oil and gas occurrence. Bull. Can. Pet. Geol. **17**(1), 47–66 (1969)
28. Utting, J.; Hamblin, A.P.: Thermal maturity of the lower carboniferous Horton group. Nova Scotia. Int. J. Coal Geol. **19**(1–4), 439–456 (1991)
29. Peters, K.E.; Cassa, M.R.: Applied source rock geochemistry. Am. Assoc. Pet. Geol. Mem. **60**, 93–120 (1994)
30. Vincent, A.J.: Palynofacies Analysis of Middle Jurassic Sediments from the Inner Hebrides. Newcastle University, Newcastle upon Tyne (1995)
31. Wilson, P.D.J.L.: The lower carboniferous Waulsortian facies. In: Wilson, J.L. (ed.) Carbonate Facies in Geologic History, pp. 148–168. Springer, Berlin (1975)
32. Abdula, R.A.; Balaky, S.M.; Nurmohamadi, M.; Piroui, M.: Microfacies analysis and depositional environment of the Sargelu

Formation (Middle Jurassic) from Kurdistan Region, northern Iraq. Donnish J. Geol. Min. Res. **1**(1), 001–026 (2015)
33. Scholle, P.A.; Ulmer-Scholle, D.S.: A color guide to the petrography of carbonate rocks: grains, textures, porosity, diagenesis, AAPG Memoir 77, vol. 77. AAPG, Tulsa (2003)
34. Cantrell, D.L.: Cortical fabrics of Upper Jurassic ooids, Arab Formation, Saudi Arabia: implications for original carbonate mineralogy. Sediment. Geol. **186**(3–4), 157–170 (2006)
35. Cantrell, D.; Swart, P.; Hagerty, R.: Genesis and characterization of dolomite, Arab-D reservoir, Ghawar field, Saudi Arabia. Geoarabia **9**(2), 11–36 (2004)
36. Flugel, E.: Microfacies of Carbonate Rocks: Analysis, Interpretation and Application. Springer, Berlin (2004)
37. Flugel, E.: Mikrofazielle Untersuchungen in der alpinen Trias. Methoden and Probleme. Mitt. Ges. Geol. Bergbaustud **21**, 9–64 (1972)
38. Tucker, M.E.: Sedimentary Petrology. Blackwell Publishing, Hoboken (2001)
39. Leeder, M.: Upper Palaeozoic basins of the British Isles-Caledonide inheritance versus Hercynian plate margin processes. J. Geol. Soc. **139**(4), 479–491 (1982)
40. Javaux, C.: La plate-forme parisienne et bourguignonne au Bathonien terminal et au Callovien. Dynamique sédimentaire, séquentielle et diagénétique. Place et création des réservoirs potentiels. Dijon (1992)
41. Brigaud, B.; Durlet, C.; Deconinck, J.-F.; Vincent, B.; Pucéat, E.; Thierry, J.; Trouiller, A.: Facies and climate/environmental changes recorded on a carbonate ramp: a sedimentological and geochemical approach on Middle Jurassic carbonates (Paris Basin, France). Sediment. Geol. **222**(3–4), 181–206 (2009)
42. Vincent, B.; Rambeau, C.; Emmanuel, L.; Loreau, J.-P.: Sedimentology and trace element geochemistry of shallow-marine carbonates: an approach to paleoenvironmental analysis along the Pagny-sur-Meuse Section (Upper Jurassic, France). Facies **52**(1), 69–84 (2006)
43. Algeo, T.J.; Watson, B.A.: Calcite, aragonite and bimineralic ooids in Missourian (Upper Pennsylvanian) strata of Kansas: stratigraphic and geographic patterns of variation. In: Carbonate facies and sequence stratigraphy: practical applications of carbonate models (A symposium). Soc. Econ. Paleont. Miner. Publ., Permian Basin Section 1995, pp. 95–36 (1995)
44. Heydari, E.; Moore, C.H.: Paleoceanographic and paleoclimatic controls on ooid mineralogy of the Smackover Formation, Mississippi salt basin; implications for Late Jurassic seawater composition. J. Sediment. Res. **64**(1a), 101–114 (1994)
45. Land, L.; Behrens, E.; Frishman, S.: The ooids of Baffin Bay, Texas. J. Sediment. Res. **49**(4), 1269–1277 (1979)
46. Sandberg, P.A.: New interpretations of Great Salt Lake ooids and of ancient non-skeletal carbonate mineralogy. Sedimentology **22**(4), 497–537 (1975)
47. Sumner, D.Y.; Grotzinger, J.P.: Numerical modeling of ooid size and the problem of Neoproterozoic giant ooids. J. Sediment. Res. **63**(5), 974–982 (1993)
48. Swirydczuk, K.: Mineralogical control on porosity type in Upper Jurassic Smackover ooid grainstones, southern Arkansas and northern Louisiana. J. Sediment. Res. **58**(2), 339–347 (1988)
49. Tucker, M.E.; Wright, V.P.: Carbonate Sedimentology. Blackwell Publishing Company, Oxford (1990)
50. Frey, R.W.; Howard, J.D.: A profile of biogenic sedimentary structures in a Holocene Barrier Island-Salt Marsh Complex. Georgia **1**, 427–444 (1969)
51. Reading, H.: Sedimentary Environments and Facies. Blackwells, Oxford (1986)
52. Reineck, H.; Singh, I.: Der Golf von Gaeta (Tyrrhenisches Meer); III, Die Gefuege von Vorstrand-und Schelfsedimenten. Senckenberg. Maritim. **3**, 185–194 (1971)
53. Tucker, M.E.: Sedimentary Petrology: An Introduction. Geoscience Texts, vol. 252. Wiley, Oxford (1981)
54. Torrent, J.; Schwertmann, U.: Influence of hematite on the color of red beds. J. Sediment. Res. **57**(4), 682–686 (1987)
55. Glennie, K.: Desert sedimentary environments, present and past—a summary. Sediment. Geol. **50**(1–3), 135–165 (1987)
56. Turner, P.: Continental Red Beds, vol. 29. Elsevier, Amsterdam (1980)
57. van Houten, F.B.: Iron and clay in tropical savanna alluvium, northern Colombia: a contribution to the origin of red beds. Geol. Soc. Am. Bull. **83**(9), 2761–2772 (1972)
58. Fürsich, F.; Oschmann, W.; Singh, I.; Jaitly, A.: Hardgrounds, reworked concretion levels and condensed horizons in the Jurassic of western India: their significance for basin analysis. J. Geol. Soc. **149**(3), 313–331 (1992)
59. Verma, D.; Jadhav, G.; Biswal, T.; Jena, S.; Sharma, N.: Characterization of hydrocarbon-bearing fluid inclusion in sandstones of Jaisalmer Basin, Rajasthan: a preliminary approach. J. Geol. Soc. India **80**(4), 505–514 (2012)
60. Srivastave, N.; Ranawat, T.S.: An overview of Yellow Limestone deposits of the Jaisalmer Basin, Rajasthan, India. Volumina Jurassica **13**(1), 107–112 (2015)
61. Zadan, K.; Arbab, K.A.: A review on lithostratigraphy and biostratigraphy of Jaisalmer Basin, Western Rajasthan, India. Int. Res. J. Earth Sci. **3**, 37–45 (2015)
62. Wang, Z.: The distribution of Mesozoic sediments in the north of Qaidam basin. Pet. Explor. Dev. **8**(2), 20–26 (1981)
63. Ritts, B.D.; Biffi, U.: Mesozoic Northeast Qaidam Basin: Response to Contractional Reactivation of the Qilian Shan, and Implications for the Extent of Mesozoic Intracontinental Deformation in Central Asia, pp. 293–316. Memoirs Geological Society of America, Boulder (2001)
64. Ritts, B.D.; Hanson, A.D.; Zinniker, D.; Moldowan, J.M.: Lower-Middle Jurassic nonmarine source rocks and petroleum systems of the northern Qaidam basin, northwest China. AAPG Bull. **83**(12), 1980–2005 (1999)
65. Qiang, J.; Ming, Z.; Zhen, L.; XianZhi, G.; Dehua, P.; Lamei, L.: Geology and geochemistry of source rocks in the Qaidam Basin, NW China. J. Pet. Geol. **25**(2), 219–238 (2002)
66. Yang, Y.; Ritts, B.; Zou, C.; Xu, T.; Zhang, B.; Xi, P.: Upper triassic-middle jurassic stratigraphy and sedimentology in the NE Qaidam Basin, NW China: petroleum geological significance of new outcrop and subsurface data. J. Pet. Geol. **26**(4), 429–449 (2003)
67. Hendrix, M.S.; Brassell, S.C.; Carroll, A.R.; Graham, S.A.: Sedimentology, organic geochemistry, and petroleum potential of Jurassic coal measures: Tarim, Junggar, and Turpan basins, northwest China. AAPG Bull. **79**(7), 929–958 (1995)
68. Ercegovac, M.; Kostić, A.: Organic facies and palynofacies: nomenclature, classification and applicability for petroleum source rock evaluation. Int. J. Coal Geol. **68**(1), 70–78 (2006)
69. Al-Agaili, H.E.C.: Palynofacies and Hydrocarbon Potential for Selected Samples from Subba Oil Field, South Iraq. University of Baghdad, Baghdad (2012)
70. Singh, H.; Mahesh, S.: Palynofacies characterization for evaluation of hydrocarbon source rock potential of Lower Paleogene (Thanetian-Ypresian) sub-surface sediments of Barmer Basin, western Rajasthan, India. Mar. Pet. Geol. **59**, 442–450 (2015)
71. Pross, J.; Pletsch, T.; Shillington, D.J.; Ligouis, B.; Schellenberg, F.; Kus, J.: Thermal alteration of terrestrial palynomorphs in mid-Cretaceous organic-rich mudstones intruded by an igneous sill (Newfoundland Margin, ODP Hole 1276A). Int. J. Coal Geol. **70**(4), 277–291 (2007)
72. Hakimi, M.H.; Abdullah, W.H.; Shalaby, M.R.; Alramisy, G.A.: Geochemistry and organic petrology study of Kimmeridgian organic-rich shales in the Marib-Shabowah Basin, Yemen: origin

and implication for depositional environments and oil-generation potential. Mar. Pet. Geol. **50**, 185–201 (2014)
73. Zhang, M.; Ji, L.; Wu, Y.; He, C.: Palynofacies and geochemical analysis of the Triassic Yanchang Formation, Ordos Basin: implications for hydrocarbon generation potential and the paleoenvironment of continental source rocks. Int. J. Coal Geol. **152**, 159–176 (2015)
74. Mirzaloo, M.; Ghasemi-Nejad, E.: Combined use of palynology and organic geochemistry in petroleum potential evaluation and paleoenvironmental interpretation of the Kazhdumi Formation (Aptian-Cenomanian) in the southwestern Zagros Basin, Iran. Geopersia **2**(1), 27–40 (2012)
75. Peters, K.E.: Guidelines for evaluating petroleum source rocks using programmed pyrolysis. Am. Assoc. Pet. Geol. Bull. **70**, 318–329 (1986)
76. Tissott, B.P.; Welte, D.H.: Petroleum Formation and Occurrence, 2nd edn. Springer, Berlin (1984)
77. El Nady, M.M.; Ramadan, F.S.; Hammad, M.M.; Lotfy, N.M.: Evaluation of organic matters, hydrocarbon potential and thermal maturity of source rocks based on geochemical and statistical methods: case study of source rocks in Ras Gharib oilfield, central Gulf of Suez, Egypt. Egypt. J. Pet. **24**(2), 203–211 (2015)
78. Ghori, K.; Haines, P.: Paleozoic petroleum systems of the Canning Basin, Western Australia: a review. American Association of Petroleum Geologists, Search and Discovery Article(10120), p. 7 (2007)
79. Rabbani, A.; Kamali, M.: Source rock evaluation and petroleum geochemistry, offshore SW Iran. J. Pet. Geol. **28**(4), 413–428 (2005)
80. Hunt, J.M.: Petroleum Geochemistry and Geology, vol. 2. WH Freeman, New York (1996)
81. Waples, D.: Geochemistry in Petroleum Exploration. International Human Resources Development Corporation, Boston (1985)
82. Espitalie, J.; Deroo, G.; Marquis, F.: Rock-Eval pyrolysis and its applications. Revue De L Institut Francais Du Petrole **40**(5), 563–579 (1985)
83. Dow, W.G.: Kerogen studies and geological interpretations. J. Geochem. Explor. **7**, 79–99 (1977)
84. Peters, K.E.; Cassa, M.R.: Applied Source Rock Geochemistry. Chapter 5: Part II. Essential elements (1994)